We are IntechOpen,
the world's leading publisher of
Open Access books
Built by scientists, for scientists

4,800
Open access books available

122,000
International authors and editors

135M
Downloads

Our authors are among the

154
Countries delivered to

TOP 1%
most cited scientists

12.2%
Contributors from top 500 universities

WEB OF SCIENCE™

Selection of our books indexed in the Book Citation Index
in Web of Science™ Core Collection (BKCI)

Interested in publishing with us?
Contact book.department@intechopen.com

Numbers displayed above are based on latest data collected.
For more information visit www.intechopen.com

Right Chambers Quantification in Clinical Practice: Echocardiography Compared with Cardiac Magnetic Resonance Imaging

Lucia Agoston-Coldea and Silvia Lupu

Additional information is available at the end of the chapter

http://dx.doi.org/10.5772/55832

1. Introduction

The right ventricle (RV) has its own particular morphology and functions, which are different when compared to the left ventricle (LV). In clinical practice, the right heart chambers are often overlooked, as most physicians tend to focus more on LV and left atrium (LA) morphology and functions. However, cardiac pathology is often associated with right chambers impairment, which can occur as a primary pathophysiological response to elevated pressure in the pulmonary arterial circulation associated with primary pulmonary artery hypertension [1-2], in pulmonary diseases associated with pulmonary venous or arterial hypertension [3-4], pulmonary embolism [5], but also in congenital heart disease [6]. Most often, RV dysfunction is triggered by left chamber impairment [7-9].

Right cardiac imaging is quite challenging, as there are few validated and reproducible parameters that can be employed for an accurate right atrium (RA) and RV morphology and function assessment. However, some imaging techniques are available for this purpose. Nowadays, cardiac magnetic resonance imaging (MRI) is the golden standard for right chambers evaluation [10], due to its unlimited imaging planes, higher image resolution, and the ability to calculate volumes using three-dimensional (3D) measurements. Regrettably, this type of evaluation is not available in many centres and rather expensive, requiring high quality equipment and highly trained examiners.

Although cardiac MRI is the preferred method [11], echocardiography remains a valuable alternative, as it is widely available, non-invasive, and less expensive and can be performed in all patients oblivious of associated pathology or the presence of metallic devices such as pacemakers, implanted cardioverter defibrillators, cochlear implants or drug infusion pumps.

Some studies seem to suggest that the risk usually associated with cardiac MRI in patients with pace makers and defibrillators is overestimated and that examination using magnetic fields up to 1.5 Tesla can be safe [12-13]. However, performing such an examination is not without risk and should be attempted in selected patients, with several precautions including complete resuscitation facilities and in the presence of an electrophysiologist [14]. All in all, cardiac MRI requires many precautions, in such cases, whereas echocardiography is without risk and easier to perform. Despite its major advantages, echocardiography has its limitations, mainly due to the particular morphology of the RV. The thin, trabeculated right free wall and the anterior position in the chest render RV assessment difficult [15]. Moreover, endocardial border tracing is strenuous due to the presence of trabeculations, which can be a source of error when attempting to obtain precise dimension assessment. These downfalls are limited when real-time 3D echocardiography is used, although, for the time being, end-systolic and end-diastolic RV volumes seem to be underestimated when compared to cardiac MRI measurements [16]. Some studies have shown, however, that, in spite of the difference in volume measurements, the correlation between 3D echocardiography and MRI assessment of the right ventricle ejection fraction (RVEF) is quite strong [17]. All in all, echocardiography can be very useful, provided that a complex standard protocol is followed.

2. Anatomy and physiology of the right ventricle

The RV has an anterior position in the chest and lies immediately behind the sternum. It has a triangular or crescent shape and three distinct regions with different embryological origin and electrophysiological properties. The three regions include: 1) the inlet component, 2) the apical trabecular component and 3) the outlet component [18]. The inlet component extends from the tricuspid valve insertion to the level of the papillary muscle, surrounding and supporting the tricuspid valve and the subvalvular apparatus. The trabecular component extends from the papillary muscles level to the apex and contains coarse trabeculations. The inlet and trabecular components have a common embryological origin and form a morpho-logical and functional structure called sinus. The sinus is the pivot structure for RV contraction. The outlet component, also called the infundibulum, conus or the RV outflow tract (RVOT) has its distinct embryological origin and is functionally different from the sinus. This compo-nent has a smooth surface and a minute contribution to RV output volume, and is the last cardiac structure to be activated, at end systole [19]. This region is particularly important in patients with congenital heart disease [20] and arrhythmias such as the idiopathic outflow tachycardia [21], as well as for the diagnosis of arrhythmogenic right ventricle dysplasia (ARVD), for which the left parasternal long-axis view is usually preferred [22]. All in all, each region of the RV (Figure 1) is essential in patients with cardiopulmonary disorders and should be analysed in correlation with segmental coronary vascularisation [18, 23].

RV physiology is closely linked to its anatomical properties. The thin, trabeculated free wall is adapted to the low pressures in the pulmonary circulation, its dynamics being very different from that of the LV. RV contraction is generated by the progression of a peristaltic wave which begins at the inlet and moves towards the infundibulum. RV depolarization triggers the
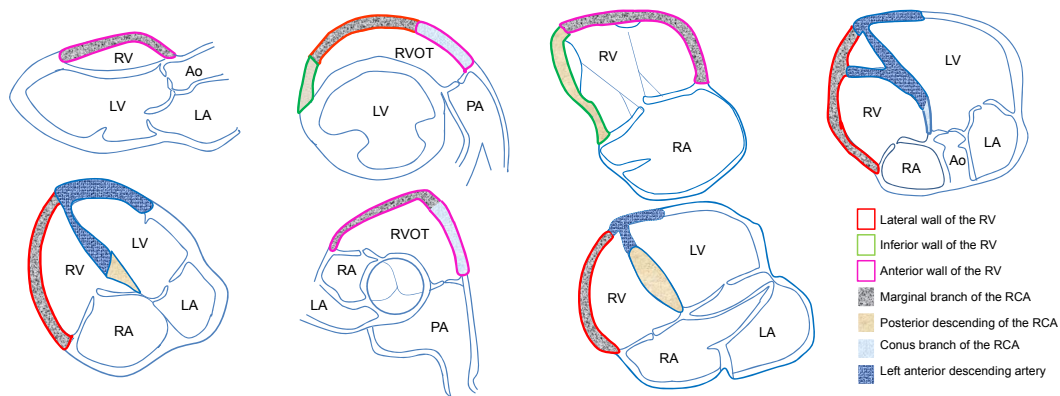
Figure 1. Segmental anatomy of right ventricle in correlation with segmental coronary vascularisation. Adapted from Rudski et al. [23]. RV=right ventricle; RVOT= right ventricular outflow tract; RA=right atrium; RCA=right coronary artery; PA=pulmonary artery; LV=left ventricle; LA=left atrium.

ance of one ventricle may influence the shape, size or pressures in the other ventricle, an essential concept for understanding the pathophysiology of RV dysfunction [9].

3. Assessment of right chambers morphology and systolic function

3.1. Echocardiography

Echocardiography can help with qualitative morphological examination by 2D and 3D echocardiography. Although 2D echocardiography is widely applied in everyday clinical practice for the morphological and functional assessment of cardiac chambers and valves, 3D echocardiography is more accurate in assessing chamber volumes, mass and functions and

provides a superior view of the valves. 2D echocardiography of the right chambers may provide diameter, area and volume measurements, which should be indexed to body surface, and allows the assessment of the systolic pulmonary artery pressure (sPAP) using the tricuspid regurgitation flow and inferior vena cava (IVC) diameter and its variations during the respiratory cycle. Newer techniques, such as tissue Doppler and strain-rate imaging, provide valuable data on the systolic and diastolic functions of the RV.

3.1.1. Right ventricle

A complete evaluation of RV structure should include the study of RV volume, shape and internal architecture, RV hypertrophy and mass, tissue characterization, assessment for potential masses [8], and regional wall motion abnormalities [26]. Normally, the RV has a crescent shape when viewed from the parasternal short-axis incidence; when the RV is submitted to pressure and volume overload, the crescent shape changes to a D shape, with subsequent septal flattening, leading to impaired LV filling and decreased output. Septal movement analysis can help distinguish between RV volume and pressure overload; in the case of volume overload, septal flattening only occurs during the diastole, whereas, in the presence of pressure overload, it is persistent throughout the entire cardiac cycle [27-28]. This phenomenon is quantitatively analyzed by deriving the eccentricity index, calculated as the RV anteroposterior over the RV septolateral diameter ratio (which may be measured at end-systole or end-diastole); a value>1 suggests RV overload and was shown to be positively correlated with pulmonary artery hypertension [29].

a. Acquisition and measurements:

Although qualitative assessment of the RV has its virtues, quantitative assessment provides more accurate and interpretable data. Morphology assessment may include diameter, area and volume measurements. RV morphology should be assessed by 2D using several acoustic windows such as the parasternal long-axis view (which allows RV anterior wall visualisation), the parasternal short-axis view (to assess the infundibulum and some of the RV anterior wall), the left parasternal RV inflow window (for the anterior, lateral and inferior RV walls, depending on the section level), the subcostal view (for the lateral wall and the infundibulum), the apical 4-chamber view, and apical 5-chamber view (for assessment of the RV lateral wall) [26] (Figure 2). Usually, the RV is best measured at end-diastole using the 4-chamber apical view. From this window, three dimensions can be derived: the basal diameter (the largest diameter in the basal third of the RV, usually just below the tricuspid annulus); the medial diameter (measured at the level of the LV papillary muscles); the longitudinal diameter (measured from the RV apex to the tricuspid annulus plane). RV free wall thickness is best measured from the subcostal view at the end of the diastole, using either 2D or M-mode imaging techniques; oblivious of the preferred method, measurements should exclude trabeculations, the papillary muscle, and the pericardium. RV volume and function may also be assessed by 3D transthoracic echocardiography using apical and subcostal views. Usually, four-beat images are necessary to include the entire RV, although newer techniques allow a good evaluation using a single beat, at the expense of temporal and spatial resolution [26].
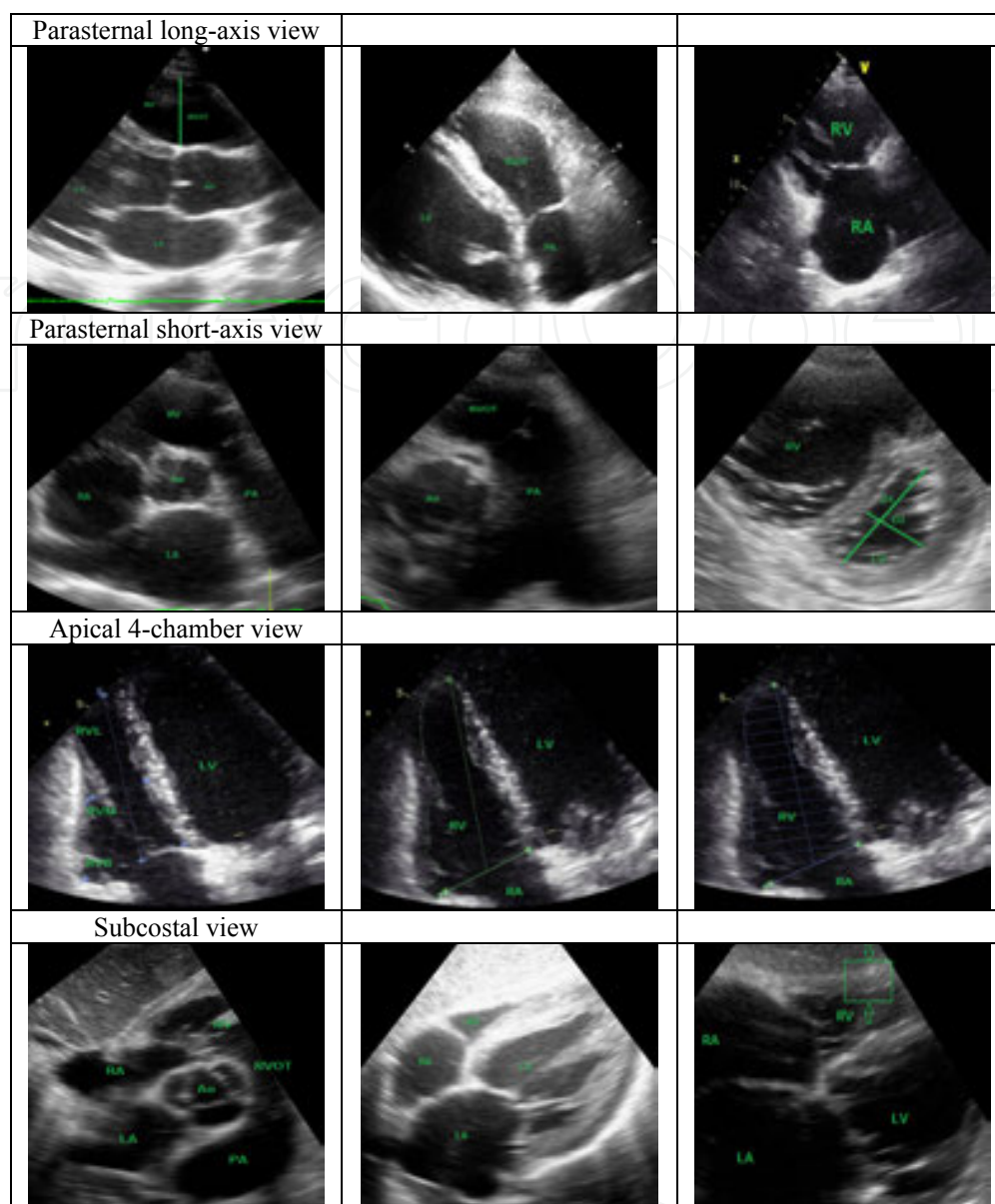
Figure 2. Echocardiography 2D views for right ventricle chamber.

Images are available for off-line analysis, allowing accurate endocardial contours delineation and RV volumes measurement from sequential long axis planes. End-diastolic measurements are taken at the peak of the R wave of QRS complexes, while end-systolic volumes are measured in the first frame before opening of the tricuspid valve [26]. Furthermore, trabeculations are included in the blood pool. The end-diastolic, end-systolic RV and stroke volume, as well as RVEF and RV mass are calculated using Simpson's rule.

b. Qualitative values:

An empirical comparison of LV and RV dimensions allows RV description as (Table 1): normal (when the RV has smaller dimensions when compared to the LV, with RV apex more basal than the LV apex); mildly dilated (when the RV is enlarged, but still smaller than the LV);

moderately dilated (when the RV and LV dimensions are equal); severely dilated (when the RV is larger than the LV) [30]. However, normal values have been established for quantitative assessment: a basal diameter >42 mm, a median diameter >35 mm and a longitudinal diameter >86 mm indicate RV dilatation. The parasternal short-axis view of the great vessels allows RVOT measurement at the level of the pulmonary valve insertion (the distal diameter) for which a value of >27 mm signifies RV dilatation. Proximal RVOT diameter can be measured from either the long or the short-axis parasternal views, with a normal maximum value of 33 mm. However, the former is usually preferred, as it is more reproducible [23]. RV areas are measured at end-diastole and end-systole, with the following normal values: RV end-diastole area 20.1 ± 4 cm^2 and RV end-systole area 10.9 ± 2.9 cm^2 [26, 30]. RV volumes may be calculated by using either the Simpson method or the area-length method and normal values range between 63-103 mL for end-diastolic volumes and 22-56 mL for end-systolic volume [31]. However, these 2D echocardiography measurements were proved to be inaccurate by comparison with 3D echocardiography and cardiac MRI derived volumes. Normal thickness ranges from 3 to 5 mm [23], and any value surpassing 5 mm suggests RV hypertrophy, which is usually a response to pressure overload, in the absence of associated pathology, such as infiltrative or hypertrophic cardiomyopathies [23].

2D echocardiography	Reference values	Mildly dilated	Moderately dilated	Severely dilated
RV dimensions				
Basal RV diameter (RVD1), mm	20-28	29-33	34-38	"/>39
Mid-RV diameter (RVD2), mm	27-33	34-37	38-41	"/>42
Base-to-apex length (RVL), mm	71-79	80-85	86-91	"/>92
RVOT diameters				
Above aortic valve, (RVOT proximal) mm	25-29	30-32	33-35	"/>36
Above pulmonic valve (RVOT distal), mm	17-23	24-27	28-31	"/>32
RV area				
RV diastolic area, cm^2	11-28	29-32	33-37	"/>38
RV systolic area, cm^2	7.5-16	17-19	20-22	"/>23
RV volume				
RV diastolic volume, mL	63–103			
RV systolic volume, mL	22–56			

Table 1. Reference limits and partition values of right ventricular size

The lack of accuracy in assessing RV volumes by 2D echocardiography is mainly determined by the complex RV geometry and the heavily trabeculated inner wall contour. Real 3D echocardiography overcomes these limitations and provides a superior evaluation of ventricular volume, mass and function, as well as a more complete view of the valves [26]. Moreover, 3D echocardiography was proved to be a reliable noninvasive modality of directing the bioptome to the desired site of biopsy within the RV. In one study, 3D echocardiography provided accurate anatomic details and was proved to allow sufficient pulmonary valve visualization in 68% of the patients and an excellent RVOT visualisation in 40% [32]. Normal medium values of RV end-diastolic and end-systolic volumes were established at 49 ± 10 and 16 ± 6 mL/m^2 respectively, with a mean RVEF of 67 ± 8% [33]. Another study provided normal reference ranges of indexed volumes: 38.6 to 92.2 mL/m^2 for RV end-diastolic volume, 7.8 to 50.6 mL/m^2 for end-systolic volume, 22.5 to 42.9 mL/m^2 for stroke volume in women and higher values in men: 47.0 to 100 mL/m^2 for RV end-diastolic volume, 14.2 to 48.4 mL/m^2 for end-systolic volume, and 23.0 to 52.6 mL/m^2 for stroke volume [34].

c. Clinical Application

The structural assessment of the RV provides information concerning the pressure and volume loading conditions which may lead to functional impairment. The RV gradually adapts to pressure overload by hypertrophy and interventricular septal flattening, with systolic function impairment, RV and tricuspid annulus enlargement and aggravated tricuspid regurgitation, which trigger RV diastolic dysfunction. Therefore, RV morphology should be assessed periodically in patients with acute or chronic respiratory pathology and valvulopathies with the purpose of identifying early anomalies which might be corrected by a proper therapeutic approach. Until recently, the eccentricity index was based on measurements made from the parasternal short-axis view, at the level of papillary muscles. However, one recent study shows that these measurements were less accurate than those made at the apical level, which was superior in terms of correlation with aggravated pulmonary hypertension [35], right chamber dilatation and RV systolic dysfunction [36]. In addition to that, ultrasound imaging techniques may identify regional morphologic abnormalities that occur in ARVD, provided the area of dysplasia is large enough. The diagnosis of ARVD is likely in the presence of significant local wall aneurysm (major diagnostic criterion), trabeculation disarray, increased thickness of the moderator band, with hyperechogenic appearance and RVOT dilatation [37]. However, despite the advantages, the diagnosis of ARVD by imaging techniques cannot rely on echocardiography alone.

3.1.2. Right atrium

The RA has its own complex pathology, as it responds to both RV volume and pressure overload. In addition to that, RA enlargement was documented in patients with atrial arrhythmias such as atrial fibrillation by both 2D and 3D echocardiography; moreover, it has been proven that RA remodelling occurs in atrial fibrillation and regresses if sinus rhythm is restored and maintained after radiofrequency catheter ablation [38]. However, RA dilatation is most often encountered in patients with elevated pulmonary hypertension.

a.   Acquisition and measurements:

The RA is most often visualized from the apical 4-chamber view or the subcostal view [23, 26, 39]. However, due to the fact that standardized data concerning RA assessment is scarce, current evaluation includes exclusively RA minimum and maximum diameter and RA area estimation. All these measurements are made by planimetry from the apical 4-chamber view, at the end of the ventricular systole, when the atrium volume is largest (Figure 3). 3D echo-cardiography, although time consuming, may also be employed to calculate RA volume, with the advantage of more accurate endocardial border tracing at end-systole. To this purpose, two orthogonal planes (two-plane), four equiangular planes (four-plane), and eight equian-gular planes (eight-plane) may be used [40]. All the collected data can be analyzed on and off-line, with cropping and threshold processing. The final result depends on the accurate and complementary use of these processing tools [41].
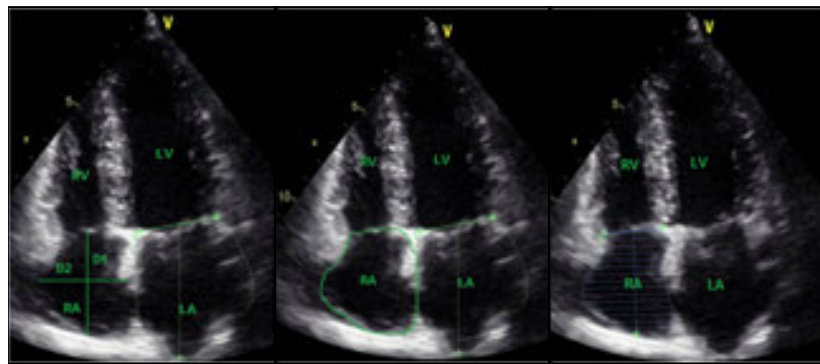

Figure 3. Echocardiography 2D views for right atrium.

b.   Qualitative values:

The maximal short-axis distance is measured at mid level, with an upper reference limit of 44 mm. The maximal long axis distance is measured from the center of the tricuspid annular plane to the center of the RA superior wall, describing a straight line parallel to the interatrial septum; the threshold for the maximal normal value has been established at 53 mm [23] (Table 2). RA area provides a more accurate assessment, but it is more time-consuming and, thusly, avoided by most physicians. The upper reference limit has been established at 18 cm^2 or at 9 cm^2/m^2. The normal RA volume indexed to body surface area is 34 mL/m^2 for men and 27 mL/m^2 for women [26, 36].

2D echocardiography	Reference values	Mildly dilated	Moderately dilated	Severely dilated
RA dimensions				
RA minor-axis dimension, mm	29-45	46-49	50-54	"/>55
RA minor-axis dimension/BSA, mm/m^2	17-25	26-28	29-31	"/>22

Table 2. Reference limits and partition values for right atrium 2D dimensions

In 3D echocardiography, RA volumes are calculated using the following formula: 0.85 (D^2)/L, where D is the area in the four-chamber view and L the vertical long-axis [42]. Images should be taken from three different beats and the loops and tracings from the first examination should be available during the second and third examination to improve accuracy (Table 3) [42].

RA 3D echocardiography	Men	Women
RAEF, %	46-74	48-83
RAVI max, mL/m^2	18-50	17-41
RAVI min, mL/m^2	7-22	5-18

Table 3. Reference limits and partition values for right atrium 3D dimensions

c.   Clinical Application

Real-time 3D echocardiography is believed to be a more reproducible and robust method for atrial volume measurements than 2D echocardiography [42], particularly in the presence of pathological conditions such as pulmonary disorders, congenital heart disease, valvular disease, and heart failure.

3.1.3. Inferior vena cava

Right chamber and pulmonary artery pressure assessment also relies on inferior vena cava (IVC) diameter measurement and the study of its variation during the respiratory cycle. In normal subjects, the IVC collapses, reducing its diameter with more than 50% after a sniff [43]; during a spontaneous, normal breathing cycle, changes in pleural pressure occur, which influence RA pressure; while inbreathing, the intrathoracic pressure becomes lower, allowing a more significant venous return and a decrease in IVC diameter. Respiratory variations are abolished in case of cardiac tamponade or severe right heart failure [43].

a.   Acquisition and measurements:

The subcostal 4-chamber view is used to measure the IVC at end-expiration, proximal to the emergence of the hepatic veins, which is usually located at 0.5 to 3 cm of the IVC-RA ostium. Maximum and minimum diameters should be measured perpendicular to the long axis of the IVC. Measurements may be facilitated by using M-mode (Figure 4).

b.   Qualitative values:

Current guidelines [23] established an upper reference limit of 21 mm for IVC diameter. For an IVC diameter ≤21 mm and an inbreathe variation of >50%, the RA pressure is estimated at 3 mmHg (range 0 – 5 mmHg). If IVC diameter is >21 mm, and the inbreathe collapse is lower than 50%, the RA pressure is estimated at 15 mmHg (range, 10 – 20 mmHg). However, some cases do not fit this paradigm; in that situation, if IVC >21 mm and significant collapse (>50%) occurs after a sniff, or if IVC ≤21 mm, but there is scarcely any inbreathe diameter variation or none at all, RA pressure is estimated at 8 mmHg (Table 4). Other authors [44] have previously

suggested a different approach (Table 4). The reference normal value interval for the IVC diameter was set at 15 – 25 mm; if the measured IVC diameter remained within these limits, and decreased with >50% after a sniff, the RA pressure was estimated at 5 – 10 mmHg; if inbreathe variation was <50%, RA pressure was estimated at 10 – 15 mmHg, and at 15 – 20 mmHg if IVC diameter was greater than 25 mm. If IVC was dilated and remained flat during the respiratory cycle, and dilated hepatic veins were also visualized, RA pressure was considered to be >20 mmHg.
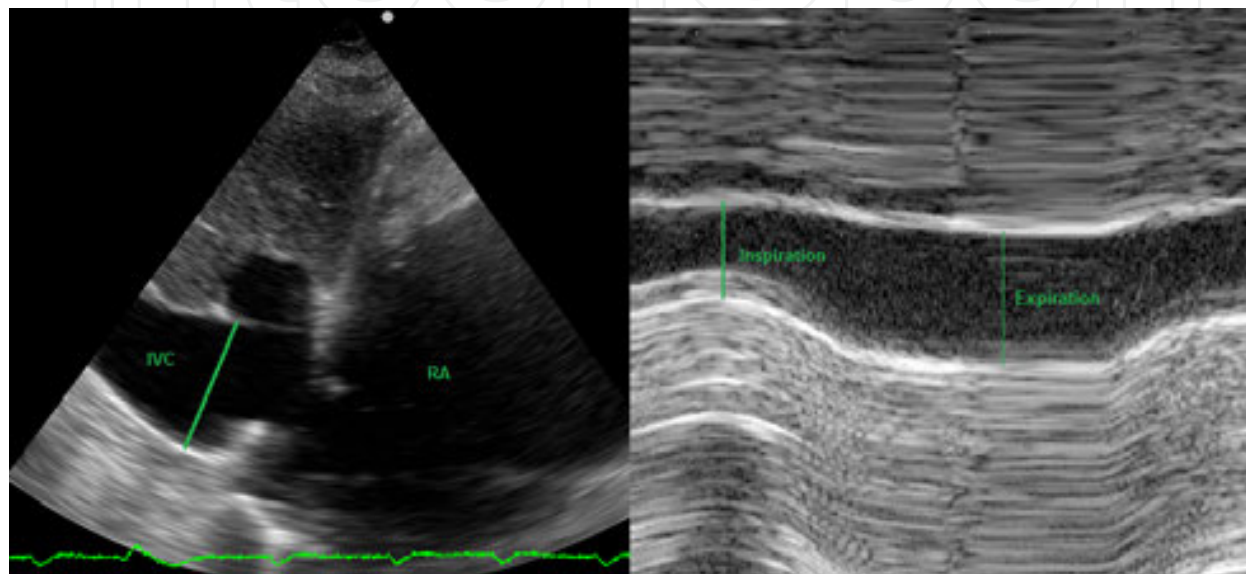

Figure 4. Measurement and view of the inferior vena cava (IVC) perpendicular to the long axis at end-expiration, just proximal to the junction of the hepatic veins that lie proximal to the ostium of the right atrium.

IVC diameter	Change after "sniff"	Estimated right atrium pressure (mmHg)
Estimated right atrium pressure by Rudski [23]		
≤ 21 mm	Collapse "/>50%	3 mmHg (range 0 – 5 mmHg)
"/> 21 mm	Collapse <50%	15 mmHg (range 10 – 20 mmHg)
"/>21 mm	Collapse "/>50%	8 mmHg (range 5 – 10 mmHg)
≤ 21 mm	Collapse <50%	8 mmHg (range 5 – 10 mmHg)
Estimated right atrium pressure by Otto [43]		
Normal range (15–25 mm)	Collapse "/>50%	5 – 10 mmHg
Normal range (15–25 mm)	Collapse <50%	10 – 15 mmHg
Dilated ("/>25 mm)	Collapse <50%	15 – 20 mmHg
Dilated ("/>25 mm)	Flat	"/> 20 mmHg

Table 4. Right atrium pressure assessment by inferior vena cava collapse and inbreathe variation

c.   Clinical Application

Oblivious of the approach, estimated RA pressure is added to the tricuspid regurgitation gradient in order to calculate the systolic pulmonary artery pressure (sPAP). Usually, IVC diameter is only used to assess sPAP, and is not interpreted individually. However, one study focused on idiopathic pulmonary hypertension patients showed that an IVC diameter ≥20 mm, with respiratory variation <50%, was a prognostic factor for mortality [45]. In some cases, such as young athletes, dehydrated patients or in the presence of mechanical respiratory assistance devices, IVC diameter correlates poorly with RA pressure.

3.1.4. Right ventricle systolic function

Assessing RV systolic function can be difficult, due to the particular morphology of the RV. Geometrical assumptions are based on pyramidal and ellipsoidal models which are not particularly accurate, as the RV has a rather irregular shape. Moreover, area and volume estimation can be impaired by the presence of trabeculations in the RV, which should be excluded from myocardial border tracings. For volume calculation, area-length and disk summation (Simpson's) methods are used, the latter being more accurate. However, volumes are underestimated by 2D echocardiography [46], when compared to 3D echocardiography [47] and cardiac MRI [34]. Cardiac computed tomography may also be used, but RV volumes tend to be overestimated using this imaging technique [48], while cardiac MRI remains the gold standard for RV assessment, although it was shown to correlate very well with real-time 3D echocardiography measurements [11]. These imaging techniques are often unavailable in most centres, rendering 2D echocardiography quite important, despite its downfalls. A complete 2D echocardiography examination should include area and volume assessment, as well as several derived parameters (Table 5), such as right ventricle fractional area change (RVFAC) and the RVEF, tricuspid annular plane systolic excursion (TAPSE), systolic velocity of the myocardium (St wave) and right ventricular myocardial performance index (RVMPI).

2D echocardiography	Reference values	Mildly dilated	Moderately dilated	Severely dilated
RVFAC, %	32-60	25-31	18-24	<17
RVEF, %	43–65	40-30	30-20	≥20
TAPSE, mm	15-20	13-15	10-12	<10

Table 5. Reference limits and partition values of right ventricular systolic function as measured in the apical 4-chamber view

a.   Right ventricle fractional area change

The RVFAC is estimated using the formula: (end-diastolic area – end-systolic area)/end-diastolic area x 100, with a lower reference value for normal RV systolic function of 35% [23] and was previously proved to diminish in primary pulmonary hypertension patients, when compared to healthy controls [49] (Figure 5). Normal RVFAC and partition values [30] are

shown in Table 5. In one study, RVFAC was found to be an independent predictor of heart failure, stroke and higher mortality in patients with prior myocardial infarction [50].
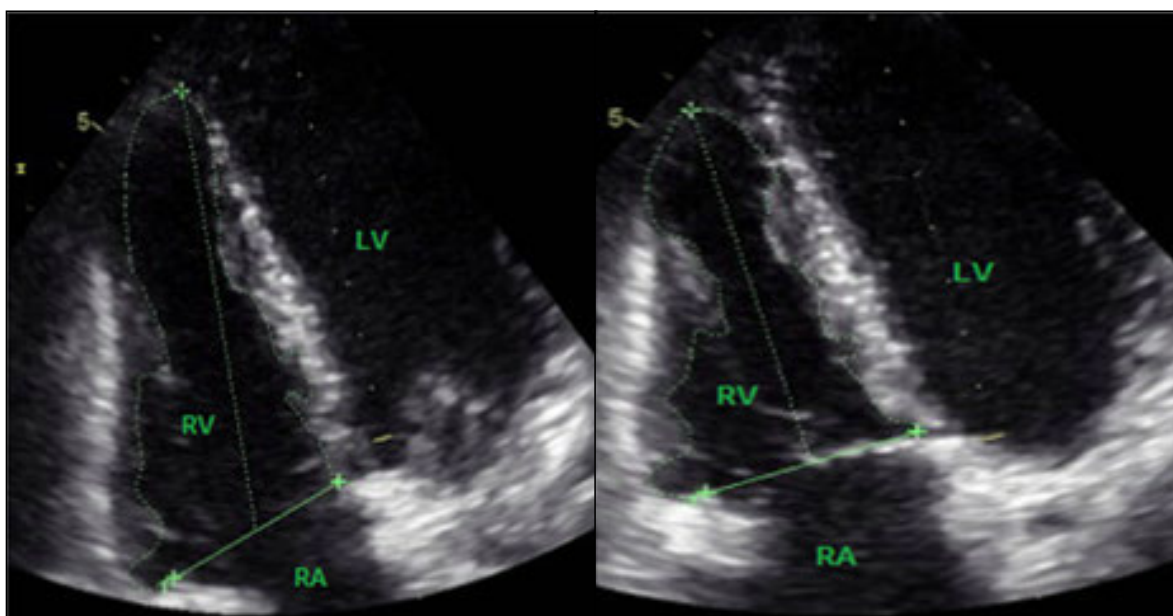

Figure 5. Measurement of the right ventricular fractional area change (RVFAC), views for right ventricle chamber.

b. Right ventricular ejection fraction

The RVEF is derived using the formula: (end-diastolic volume – end-systolic volume)/end-diastolic volume, for which the minimal normal value was established at 44% (Figure 6). Although RVEF measurement by echocardiography is impaired by geometrical assumptions, difficult endocardial border tracing and the fact that the RVOT is not included in area and volume assessment, it is still a valuable parameter, as some studies showed that RVEF is a strong and independent predictor of mortality in heart failure [51-52]. Both RVFAC and RVEF were proved to significantly correlate with other RV function parameters such as the myocardial performance index [53]. As mentioned above, the RV systolic function is dependent on the LV function and can be altered in the presence of interventricular septum movement abnormalities. The LV systolic function is mostly determined by the radial contraction, while the thin RV free wall systolic movement is predominantly determined by longitudinal shortening.

c. Tricuspid annular plane systolic excursion

To assess RV free wall systolic shortening, the TAPSE is measured. This parameter is assessed using the apex-4-chamber view and the M-mode; the cursor is placed at the level of the tricuspid annular plane, allowing the examiner to assess the base to apex motion of the annular plane during systole (Figure 7). The minimal reference threshold has been established at 16 mm (normal values ranging around 22 ± 4 mm) and it is inferred that higher TAPSE values correspond to a better systolic function. TAPSE is easy to measure, reproducible, does not
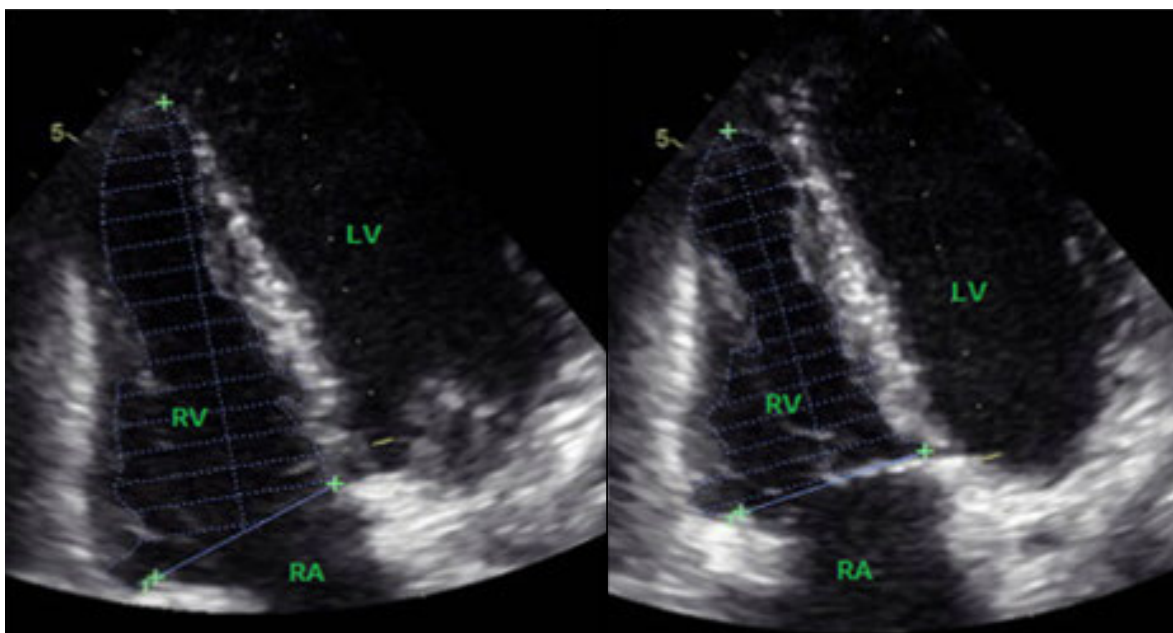
Figure 6. Measurement of the right ventricular ejection fraction (RVEF), views for right ventricle chamber.

require special equipment and is valuable when assessing RV function after myocardial infarction, but does present with some downfalls, particularly due to the fact that it only reflects the basal segment function, ignoring other regions. Moreover, it is angle and load dependant. However, some studies have shown that it correlates well with RVFAC and Simpson's method derived RVEF [35, 54], as well as ventriculography derived RVEF [24] and that it is highly reliable as a prognostic tool in pulmonary hypertension [52, 55], heart failure [24] and dilated cardiomyopathy, oblivious of the ischemic or non-ischemic aetiology [52].

Some level of correspondence has been demonstrated between TAPSE (in mm) and RVEF; a TAPSE of 5 mm corresponds to a 20% RVEF, 10 mm to a 30% RVEF, 15 mm to 40%, 20 mm to 50% [56].

d.   Tissue Doppler analysis

Tissue Doppler imaging's (TDI) may be used to obtain other indices of RV performance such as the St wave, the isovolumic contraction velocity and the derived myocardial acceleration (Figure 8) during isovolumic contraction. All these parameters are quite independent of anatomical properties and do not rely on any geometrical assumptions, but may be influenced by load conditions. As they are angle dependent, Doppler beam alignment should be optimal. The isovolumic contraction velocity is measured using either pulsed or colour-coded TDI with sample volume placement on the RV free wall at the level of the tricuspid annulus. The isovolumic contraction phase starts immediately after the A' wave corresponding to ventricular filling during atrial systole and precedes the St wave which describes ventricle wall movement during the ejection phase. In one study, the isovolumic contraction velocity was shown to correlate very well with mean RA pressure and proved to have 100% sensitivity and 78% specificity for a cut-off value <6 cm/s [57-58].
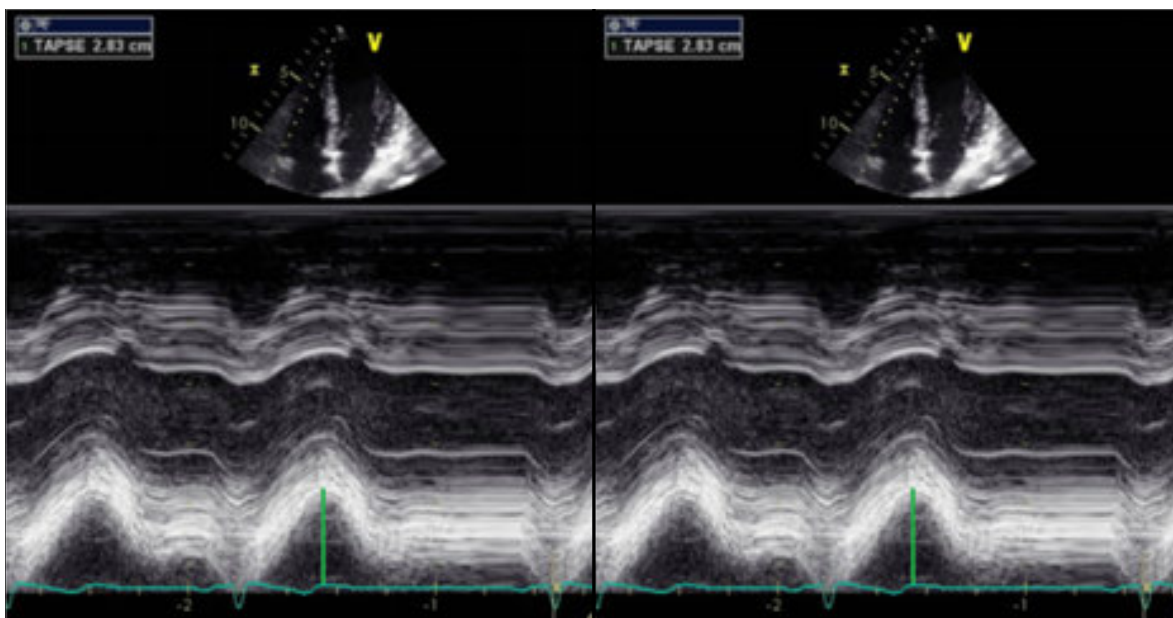
Figure 7. Measurement of the tricuspid annular plane systolic excursion (TAPSE) in normal and pulmonary artery hypertension individual, in the four chamber view a straight line (M mode) is drawn through the lateral tricuspid valve annulus.
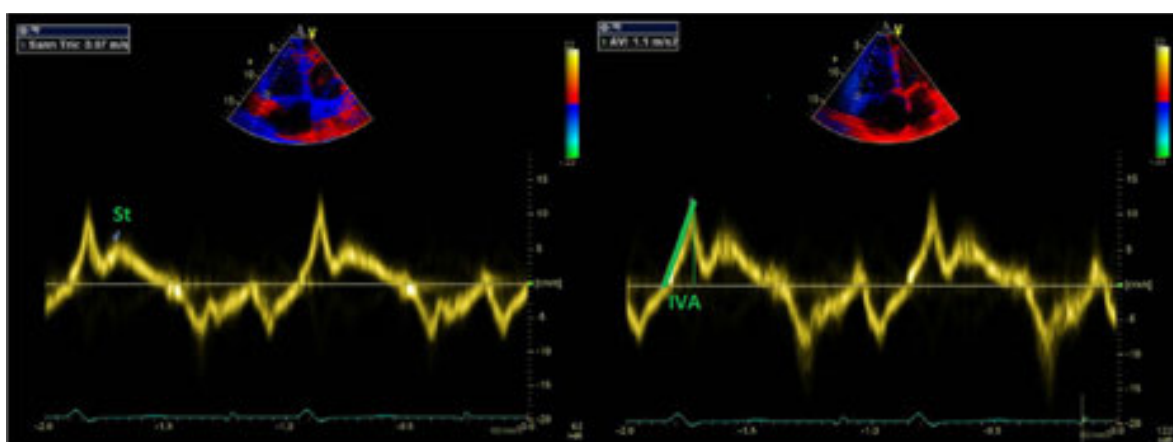

Figure 8. Pulsed wave tissue Doppler with the sample placed at the level of the tricuspid annulus of the RV free wall, demonstrating peak systolic velocity (St), and myocardial acceleration during isovolumic contraction (IVA).

This parameter may further be used to derive the myocardial acceleration during isovolumic contraction (IVA) which is calculated as the peak isovolumic contraction velocity divided by the time to peak velocity. Myocardial acceleration during isovolumic contraction may be measured either by pulsed-wave TDI or colour-coded TDI, but normal values seem to be different; in one study, values proved to be up to 20% higher when assessed by pulsed-wave TDI, by comparison with colour-coded TDI evaluation [23] [59]. In addition to that, normal values vary with age [60] and heart rate. For tissue Doppler assessment, pooled data from 10 studies established a lower reference value of 2.2 m/s [23]. IVA was studied on several animal models which lead to significant conclusions which may be implemented in every day practice.

Vogel et al. conducted a study on pigs, proving that IVA is afterload and preload independent [61], while Hashimoto et al. conducted their research on sheep, proving that IVA correlates very well with peak positive dp/dt measured invasively by right heart catheterization [62]. In humans, studies have shown that IVA was significantly correlated with disease severity in patients with chronic obstructive pulmonary disease [63], obstructive sleep apnoea [64], RV remodelling triggered by type 2 diabetes mellitus [65], and that it may be used for early detection of RV dysfunction in patients with mitral stenosis [66] or systemic sclerosis, even before the onset of pulmonary hypertension [67]. Moreover, in one study on patients who underwent corrective surgery for transposition of the great arteries, IVA was proved to be superior to the peak systolic myocardial velocity in assessing the reduction of functional reserve, in both the RV and LV [68].

TDI may also be used for measuring the highest St wave. This parameter is obtained from the apical four chamber view by positioning the sample volume either at the level of the tricuspid annulus, on the lateral wall, or in the middle or apical segments segment. The latter locations are, however, avoided by most physicians as adequate signals are rarely obtained and measurements are less reproducible, with greater interobserver variability [58]. St may be measured using pulsed tissue or colour coded TDI, and is, as other TDI parameters, angle dependent, but less influenced by loading conditions or RV anatomy when compared to other systolic function parameters. Mean annular velocities have been established at 8.5 – 10 cm/s, while basal free wall velocities are slightly higher at 9.3 – 11 cm/s [23], with lower velocities in elderly subjects due to the increased stiffness of the myocardium [60, 69, 70]. The main limitation of this parameter is determined by the fact that it only reflects changes in systolic movement of the basal segment which are extrapolated as descriptive for the systolic function of the entire RV. This type of measurement may sometimes be inaccurate in the presence of segmental RV systolic dysfunction which may occur in some clinical conditions such as RV myocardial infarction, ARVD or pulmonary embolism. A St value under 10 cm/s should rise suspicion of RV dysfunction, especially in young subjects, although a minimum reference value was established at 6 cm/s by pooled data from several studies [23]. In one research, a St value of <12 cm/s showed high sensitivity (81%), specificity (82%) and negative predictive value (92%) for the diagnosis of RV myocardial infarction [71], while Meluzin et al. demonstrated it was significantly correlated with RVEF and that a value <11.5 cm/s predicted RV systolic dysfunction with 90% sensitivity and 85% specificity in patients with heart failure [72]. Also, St was also shown to be lower, as expected, in patients with systemic sclerosis [67].

e. Right ventricular myocardial performance index

Both the systolic and diastolic functions of the RV may be evaluated using the myocardial performance index, also known as RVMPI or Tei index. This index can be obtained either by pulsed Doppler or TDI and is defined by the ratio of isovolumic time/ejection time. The ejection time is assessed by placing the pulsed Doppler cursor at the level of the RVOT and is measured from the onset to the cessation of the systolic pulmonary artery flow. When the pulsed Doppler cursor is placed at the level of the tricuspid annulus, the time from the cessation of the A wave to the onset of the next E wave is measured and the difference between this interval and the ejection time signifies the total isovolumic time (isovolumic resting time + isovolumic con-

traction time). These measurements are taken from two different acoustic windows and, implicitly, in different points in time, therefore errors can occur if the RR interval is not regular. Consequently, measurements may only be made if the rhythm is regular and are not feasible in case of atrial fibrillation. When using the TDI method, measurements are taken during a single heart beat, by placing the cursor at the level of the tricuspid annulus (Figure 9). The isovolumic contraction time (IVCT) is measured from the cessation of the At wave to the beginning of the St wave, the ejection time (ET) – from the onset to the cessation of the St wave, and the isovolumic relaxation time (IVRT) – from the end of the S' wave to the onset of the Et wave. The correlation between the tissue Doppler and pulsed Doppler methods are modest, due to differences in isovolumic times, which lead to higher cut-off points when tissue Doppler is used, as it was shown in studies focused on the LV [73, 74]. Moreover, one recent study showed that LV Tei index assessment by tissue Doppler was better correlated with the LV ejection fraction in patients with heart failure [75]. Similar results were obtained in a study on a paediatric population with congenital heart disease which showed that the TDI derived Tei index values were different from those obtained by pulsed Doppler and that they had additional utility, as they might help differentiate systolic from diastolic dysfunction by providing specific information on the isovolumetric intervals [76]. For the RVMPI, the upper reference limit has been established at 0.40 by the pulsed Doppler method and at 0.55 by the tissue Doppler method [23]. Any values above these thresholds are considered to be patho-logical, as stated by Brierre et al. who obtained a mean value of the Tei index of 0.90 in their research on idiopathic pulmonary artery hypertension patients; moreover, they showed that values ≥0.98 were associated with increased mortality [45].

Up to date, RVMPI was proved to be useful for RV function assessment in several studies. One study on patients with acute RV myocardial infarction showed that the Tei index was valuable for diagnosis, RV function quantification and, interestingly, for acute improve-ment assessment [77].

In another research by Blanchard et al. conducted on patients with chronic thromboembolic pulmonary hypertension, RVMPI was shown to be a valuable tool for monitoring disease severity and for assessing outcome after pulmonary thrombo-endarterectomy, and positively correlated with pulmonary vascular resistance, measured by right heart catheterization [78]. Moreover, RVMPI was shown to be a high sensitivity and specificity parameter for diagnostic purposes in patients with acute pulmonary embolism, as well as a valuable tool for assessing the response to efficient anticoagulant therapy [79-81]. In addition to that, Haddad et al. demonstrated that both the RVMPI and the RVFAC may have an incremental prognostic value in terms of mortality and morbidity after valvular heart surgery [82], while others confirmed its utility in assessing global RV function in children with congenital heart disease [83-84]. The Tei index also proved its value in RV function assessment in patients with sleep apnoea, as it was positively correlated with the anoxia-hypoxia index, while RVFAC showed inverse correlation with the same parameter [85].

The echocardiographic evaluation of RV by RVMPI has many advantages, as it is non-invasive, widely available, reproducible and independent of any geometric assumptions. If the pulsed wave Doppler method is used, errors may occur if the RR interval is variable. This downfall

may, however, be limited by using the tissue Doppler method which allows measurement taking during a single heart beat, but results are still unreliable in patients with atrial fibrillation. Other disadvantages include load dependency and altered results when RA pressure is elevated, due to artificial IVRT shortening which leads to lower RVMPI values [86].
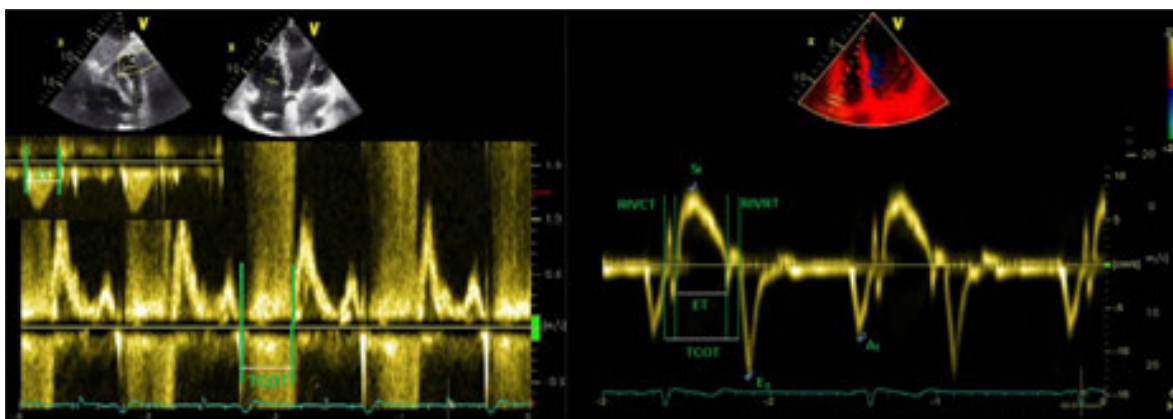

Figure 9. Measurement of right ventricular myocardial performance index (RVMPI) by pulsed wave Doppler of tricuspid regurgitation and tissue Doppler with the sample placed at the level of the tricuspid annulus of the RV free wall.

f.   Analyzing the tricuspid regurgitation flow

RV systolic function assessment can also be performed by analyzing the tricuspid regurgitation flow, which is commonly visualized from the apical 4-chamber view. Using continuous-wave Doppler, several parameters can be derived, such as: RV-RA pressure gradient, systolic, diastolic and mean pulmonary artery pressure (sPAP; dPAP; mPAP), the rate of pressure rise in the RV (dp/dt), and the previously described right index of myocardial performance (RVMPI). To this purpose, an optimal parallel alignment of the continuous Doppler cursor to the tricuspid regurgitation (TR) flow should be obtained. The rate of pressure rise in the RV (dp/dt) was first described in 1962 and measured invasively by right heart catheterization. An echocardiographic method based on the Bernoulli equation was developed to serve the same purpose, although it was shown that continuous-wave Doppler analysis of the TR flow significantly underestimated peak RV pressures when compared to invasive measurements [87]. The rate of pressure rise is calculated by measuring the time interval in which the tricuspid flow velocity rises from 1 m/s to 2 m/s (Figure 10). Based on the Bernoulli equation, this rise in velocity corresponds to a pressure elevation of 12 mmHg. Other researchers suggest that dp/dt assessment correlates better with invasive measurements if the studied time interval is focused on a rise in velocity from 0.5 to 2 m/s, which corresponds to a 15 mmHg rise in pressure [88]. The value of dp/dt is expressed in mmHg/sec, but normal reference values have not been established so far; this parameter, although easy to obtain, has limited clinical value, also due to the fact that it is load and angle dependent. However, values <400 mmHg/s are likely to be abnormal [23]. One small study showed that the dp/dt over maximum RV pressure ratio had a significant correlation to the NYHA functional class, while dp/dt by itself had none at all [89]. Nowadays, this parameter is of little interest.
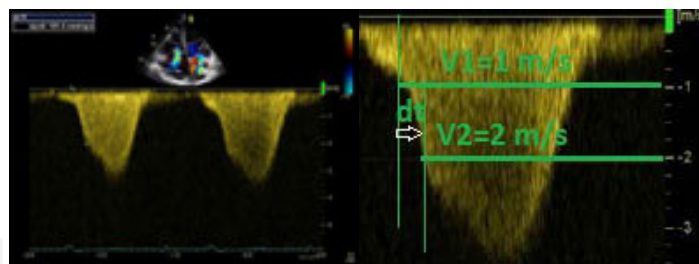
Figure 10. Measurement of the rate of pressure rise in the ventricles (dp/dt) of tricuspid regurgitation in the four chamber view in pulmonary artery hypertension individual.

The RV-RA pressure gradient may also be estimated using the peak velocity of the TR flow based on the simplified Bernoulli equation: peak pressure gradient of TR= 4 x (TR maximum velocity)^2. As it is angle dependant, the best possible alignment of the continuous-wave Doppler cursor with the regurgitation jet should be obtained and several measurements, from several acoustic windows (most often, apical 4 chamber view and parasternal RV inflow view), should be taken (Figure 11). The signal with the highest velocity and density should be used; the Doppler signal may be enhanced by injecting agitated saline into the venous flow. Moreover, special attention is necessary to exclude RVOT obstruction, which often occurs in congenital heart disease. sPAP is then calculated by adding the estimated RA pressure (assessed by IVC diameter and its inbreathe variations, as described above) to the RV-RA gradient.
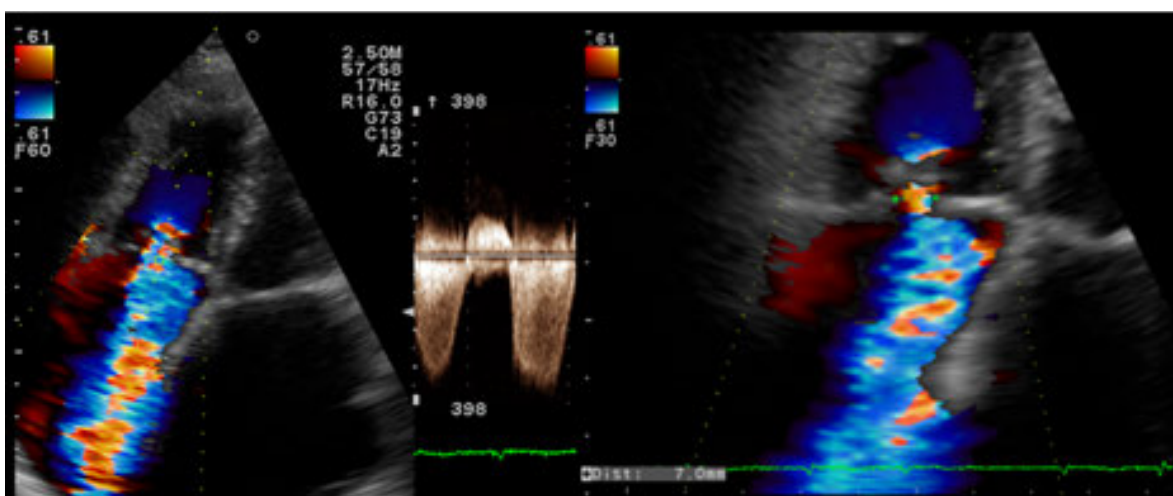

Figure 11. Doppler echocardiographic determination of systolic pulmonary artery pressure (sPAP).

A tricuspid regurgitation jet maximum velocity of ≤ 2.8 m/s renders pulmonary hypertension unlikely, a velocity of >3.4 m/s – likely, while values between 2.8 m/s and 3.4 m/s indicate that pulmonary hypertension is possible [90-91]. Normal resting values have been established at ≤36 mmHg for peak systolic pressure, assuming a RA pressure of 3-5 mmHg [23, 92].

The severity of pulmonary hypertension may be underestimated in the presence of severe tricuspid regurgitation that leads to elevated RA pressure and, consequently, to a lesser RV-RA pressure gradient and lower sPAP (Table 6).

	TR maximum velocity	PAPs	Other echo parameters suggesting HTP*
PH unlikely	≤ 2.8 m/s	≤ 36 mmHg	
PH possible	≤ 2.8 m/s	≤ 36 mmHg	+
	2.9 – 3.4 m/s	37 – 50 mmHg	+/-
PH likely	>3.4 m/s	>50 mmHg	

* dilated right chambers; increased thickness of the RV free wall; abnormal shape and function of the interventricular septum; dilated pulmonary artery; increased velocity of the pulmonary regurgitation jet; short acceleration time of RV ejection in the pulmonary artery; PH - pulmonary hypertension

Table 6. Arbitrary criteria for the presence of pulmonary hypertension based on continuous Doppler derived systolic pulmonary artery pressure (sPAP) and tricuspid regurgitation (TR) jet maximum velocity [90].

Like the sPAP, the dPAP can be derived by applying the Bernoulli equation to the pulmonary regurgitation flow: dPAP=4 x (end-diastolic regurgitant velocity)^2 + RA pressure. The pulmonary regurgitation flow may also be used to calculate the mPAP pressure after the same principle, by the formula mPAP= (4 x early PR velocity) + RA pressure, or by adding RA pressure to the velocity time integral (VTI) of the tricuspid regurgitation, the latter method being the most accurate, as it correlates better to invasive measurements by right heart catheterization [93, 94]. Previous methods relied on more vague estimations, based on the sPAP and dPAP: mPAP= 1/3 sPAP + 2/3 dPAP, or obtained by analysing the pulmonary artery continuous wave Doppler flow, using the formula mPAP= 79 – (0.45 x AT) (AT= acceleration time) [95].

The AT is measured from the onset of the pulmonary flow, which corresponds to the onset of the QRS complex on the ECG, to the onset of the maximum pulmonary velocity; consequently, the shorter the AT, the higher the mPAP. This formula applies when the heart rate is between 60 and 100 bpm, and the AT is below 120 msec. A study showed, however, that, in case of aggravated pulmonary hypertension, when AT shortens below this threshold, the formula mPAP= 90 – (0.62 x AT) led to more accurate results [95]. Despite the technical progress and reasonable mathematical and physical assumptions, right chamber and pulmonary pressure assessment by echocardiography is not sufficient for diagnosing pulmonary hypertension. In pulmonary artery hypertensive patients, right heart catheterisation remains the golden standard [94], as it is needed to confirm the diagnosis, to assess severity and to test for vessel reactivity if specific therapy is considered [90]. Several studies have shown that sPAP is considerably underestimated by echocardiography when compared to right heart catheterization, oblivious of the used method [96-98]. However, despite all the limitations, the assessment of pulmonary artery pressures by echocardiography can be used as a screening method for pulmonary hypertension [90, 94].

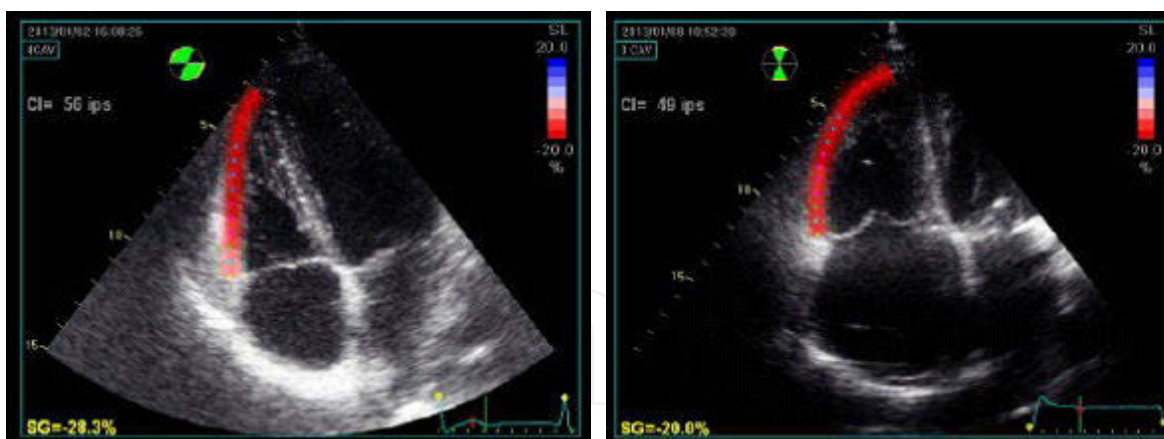**g.** Regional RV Strain and Strain Rate

Figure 12. Measurement of global right ventricular deformation by speckle-tracking with the sample placed at the level of the RV free wall in normal and pulmonary artery hypertension individual.

Strain and strain rate (SR) imaging can provide valuable data on the relative deformation of myocardial segments under stress. The resting length of the myocardium (L0) changes when submitted to a certain force (L1). Myocardial strain is best described by the L1-L0/L0 ratio, expressed in a certain percentage, which is negative when shortening occurs and positive when the myocardium lengthens. The SR can be derived using strain and the velocity of myocardial deformation, expressed in 1/s. The particular anatomy of the RV, which is mainly composed of longitudinal and oblique fibres, renders it highly susceptible to strain variations at lower stress when compared to the LV [99]. Right myocardial velocities are, thusly, higher than in the LV and more elevated at the apex, when compared to the base, even in normal individuals [99].

TDI-derived and speckle-tracking echocardiography-derived strain and SR can be used to assess RV dynamics and were found to be both feasible and roughly comparable. Strain and SR correlate well with radionuclide RVEF [24].

Normal strain is 19 ± 6 % in the basal RV free wall, 27 ± 6 %, in the median and 32 ± 6 % at the apex for the prediction of RVEF >50% [100]. This renders strain assessment of the RV quite strenuous, with important limitations due to the need of perfect alignment of the TDI cursor to the rather thin free wall of the RV. In addition to that, strain analysis is highly dependent on hemodynamic variations [101]. In patients with RV disease or dysfunction, peak systolic strain and SR are significantly reduced and delayed compared with individuals with normal RV function [24].

RV speckle-tracking is less challenging in terms of angle issues, provided that optimal endocardial border tracking is performed [102]. In 2D speckle-tracking analysis, a certain selected zone is studied in motion, allowing a good assessment of the longitudinal, radial and torsion movements of the RV (Figure 12); however, this method is limited by a low temporal resolution [102].

h.   3D echocardiography

3D echocardiography may also be used to assess right ventricle systolic and diastolic functions. It has been previously demonstrated that 3D echocardiography-derived RVEF correlated

negatively with 2D-derived pulmonary arterial systolic pressure and positively with TAPSE, the peak systolic velocity, and the fractional shortening area [32]. In one study, patients with mitral valve prolapse who underwent surgical treatment had significantly lower TAPSE and peak systolic velocities of the tricuspid annulus after surgery, while 3D-derived RVEF remained the same (58.4 ± 4%) [32]. Moreover, 3D echocardiography analysis was used to describe RV systolic function in patients with various cardiovascular disorders, showing that patients with pulmonary hypertension had the largest RV volumes and RVEF, while those with idiopathic dilated cardiomyopathy had considerably lower RVEF when compared to patients with valvular heart disease [32].

In another study, normal RVEF reference values were established at 38.0% to 65.3% for women and 29.9% to 58.4% for men [34].

3.2. Cardiac magnetic resonance imaging

Nowadays, cardiac MRI is considered to be the gold standard for determining RV volume and function [11]. This method should be taken into account when 3D echocardiography is not sufficient for evaluation.

a.   Acquisition and measurements:

Cardiac MRI requires a minimum 1.5 Tesla scanner, with a phased-array cardiac coil. Cine imaging acquired 2-chamber and 4-chamber views allow the positing of a retrospectively ECG-gated steady-state free procession pulse sequence using following parameters: repetition time 3.5–4.2 ms, echo time 1.5–1.8 ms, flip-angle 45°, matrix 256 × 256, field of view 250–350 mm, slice thickness 5–8 mm with a gap of 0–2 mm depending on body size; 12 slices should be acquired [10]. Cardiac MRI allows an accurate delineation of the endocardial and epicardial borders in all planes and all cardiac phases; in addition to that, the systolic descent and twist of the tricuspid valve is quantified by tracking of the valve motion on the long-axis cines in order to correct for loss of systolic RV volume due to AV ring descent; thirdly, papillary muscles are delineated, with blood pool thresholding. This technique allows the calculus of RV end-systolic and end-diastolic volumes, RV ejection fraction and right ventricular mass with a great degree of precision [103-104]. Cardiac MRI allows a complete assessment of the RV inflow and outflow, regardless of ventricular size or shape. The extent of myocardial damage or fibrosis is evaluated using late gadolinium enhancement.

b.   Qualitative values:

Several reference values for RV volumes have been mentioned, with significant gender differences; consequently, larger RV volumes were documented in males when compared to females: RV end-diastolic volume 190 ± 33 mL vs. 148 ± 35 mL, RV end-systolic volume 78 ± 20 mL vs. 56 ± 18 mL [105]. Other values were obtained in another study, which compared MRI-derived volumes against 3D echocardiography volumes, proving the former were larger. The following mean normal values were established for RV end-diastolic, end-systolic, and stroke volumes: 134.2 ± 39.2 mL vs. 124.0 ± 34.4 mL; 69.7 ± 25.5 mL vs. 65.2 ± 23.5 mL; and 64.5 ± 24.1 mL vs. 58.8 ± 18.4 mL [106].
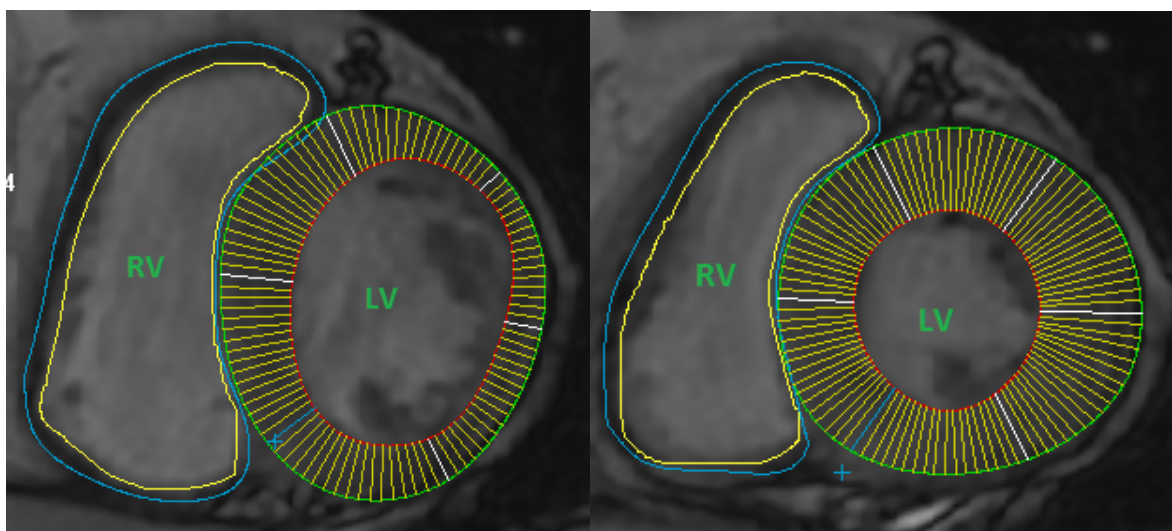
Figure 13. Cardiac MRI steady-state free procession sequence for the assessment of right ventricular function en-diastolic and en-systolic. RV=right ventricle; LV=left ventricle.

c.   Clinical Application

The efficiency of 3D echocardiography vs. cardiac MRI in RV assessment was compared in many studies. One research group conducted a study on 60 pulmonary artery hypertensive patients [4], proving that 3D echocardiography had some advantages over cardiac MRI, as it could be routinely used for serial imaging and at the bedside. Moreover, it was previously shown that both 3D echocardiography and cardiac MRI may be used to assess RV remodeling in pulmonary artery hypertension patients [11, 34, 107]. However, cardiac MRI results proved to be more reproducible in terms of assessing RV ejection fraction and RV mass [26]. Although less available, cardiovascular MRI is frequently used nowadays to describe RV systolic function; recent imaging techniques allow a good assessment of parameters such as ventricular volumes, ejection fraction, and myocardial mass, with increased accuracy when compared to echocardiography. Stroke volumes, cardiac output, and volumes routed through cardiac shunts can be derived using flow velocities and cross sectional areas. These methods are similar to those used in Doppler echocardiography, but provide a better accuracy, as MRI velocity analysis can be conducted in any orientation or plane. Tissue parameters are best visualized by contrast enhancement techniques (contrast-enhanced MRI), which typically use gadolinium-based magnetic contrast agents [103]. Similar to strain echocardiography, tagged MRI is used to study the 3-dimensional motion and deformation in the heart. Tags are regions of the myocardium, whose longitudinal magnetization has been altered before imaging which render them dark in MRI. These dark areas are landmarks within the heart which allow the detection of motion. In one study on patients with idiopathic pulmonary arterial hypertension, tagged MRI was used to identify significant interventricular asynchrony caused by a prolonged RV systolic contraction time, probably due to impaired electrical conductivity in the right ventricle. It was then showed that ventricular asynchrony led to impaired LV diastolic filling and, consequently, to decreased LV end-diastolic volumes [108]. Although further research would be needed to validate reproducible parameters for RV evaluation, echocar-

diography and cardiac MRI based techniques are, for the time being, of immense value. As mentioned before, cardiovascular MRI is nowadays considered to be the gold standard for RV assessment; in one research, some 3D echocardiography-derived measurements, such as the RVEF, compared well against cardiac MRI results, with little difference ($47.8 \pm 8.5\%$ vs $48.2 \pm 10.8\%$) [106]. However, in another study, a tendency to overestimate RVEF by 3D echocardiography, with a bias of approximately 13% (95% CI -52% to +27%), has been reported; moreover, in the same research, RV diastolic and RV systolic volumes were shown to be systematically and significantly underestimated by 3D echocardiography [109]. Solid correlations were established between 2D echocardiography tissue Doppler St wave velocity and MRI-derived RVEF [110]. In addition to that, it was shown that a systolic long-axis peak velocity of <11 cm/s at the lateral tricuspid annulus was associated with moderately impaired MRI-derived RVEF, while severely reduced RVEF ≤30% was best detected by RVMPI at a value of >0.50 [111].

4. Assessment of right ventricular diastolic dysfunction

4.1. Echocardiography

4.1.1. Tissue Doppler analysis

a.   Acquisition and measurements:

The assessment of RV diastolic dysfunction strongly resembles LV evaluation. Validated parameters include the tricuspid flow E and A velocities, as well as the E/A ratio, the E wave deceleration time and the IVRT, which are assessed in a similar manner to mitral flow evaluation; the previously mentioned parameters are measured using the apical 4-chamber view by placing sample volume at the tips of the tricuspid leaflets.

Several limitations undermine the accuracy of tricuspid flow parameters, particularly the preload and afterload dependency. Preload variations are significant during the respiratory cycle due to fluctuant intrathoracic pressure, which is diminished during inbreathing and rises during expiration. Low intrathoracic pressure favours venous return to the RA, leading to better atrial filling and increased pressure; as a consequence, early diastolic ventricular filling is improved, with an increase in E wave velocity, while A wave velocities remain almost the same; subsequently, the E/A ratio may change. Conversely, lower E wave velocities are obtained when preload decreases during expiration. This is why some authors suggest that at least 5 beats should be analysed in each patient in order to obtain an average value that should have clinical significance [112]. Other physiological factors that influence tricuspid flow patterns are age, gender and tachycardia [112]. Measurements may also be altered by the presence of severe tricuspid regurgitation or atrial fibrillation [23]. Moreover, the thin-walled RV is also highly sensitive to afterload variations, particularly in patients with myocardial infarction or chronic ischemia [113]. TDI is another valuable tool for assessing RV diastolic function. TDI is used to measure velocities at the level of the tricuspid annulus (Et, At, Et/At) and to derive the E/Et ratio which is gaining interest as a marker of diastolic dysfunction. In

clinical practice, both pulsed and colour TDI may be used; the former technique is simpler and provides a high temporal resolution, but is hindered by low spatial resolution [114]; the latter has high spatial resolution, but lower temporal resolution and provides mean velocities [115], as opposed to pulsed TDI, by which maximum velocities are measured. Although considered superior to pulsed wave Doppler techniques, TDI measurements have their limitations. Firstly, like pulsed Doppler parameters, they are influenced by age and gender [116].
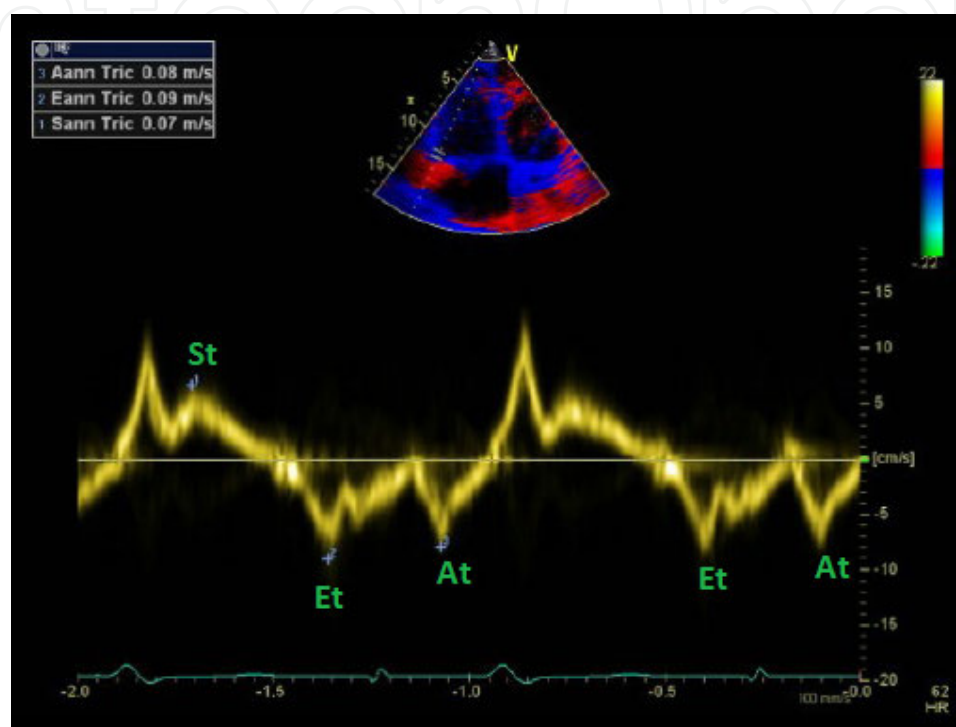

Figure 14. Pulsed wave tissue Doppler with the sample placed at the level of the tricuspid annulus of the RV free wall, demonstrating diastolic parameters (Et and At).

b. Qualitative values:

Moreover, although previous studies focused on the LV supported TDI load independency [117], Pelà et al. demonstrated in their research on healthy subjects that RV Et and At wave velocities were dependent on loading conditions; however, they also showed that Et and At velocity variations were proportional, and consequently, despite alterations in preload, the Et/At ratio remained constant. [118]. According to Horton et al., measuring parameters from ≥ 3 different beats during apnoea may reduce errors derived from load variations and the translational motion of the myocardium [119]. Despite the limitations, several researches have confirmed that pulsed and tissue Doppler allow a clinically significant evaluation of RV diastolic function. Puwanat et al. demonstrated that a tricuspid E/Et ratio >6 was associated with a mean right atrium pressure >10 mmHg in patients with heart failure and preserved ejection fraction [120]; this finding was consistent with data from a previous research by Utsunomyia et al. who demonstrated that intraatrial pressure assessment by use of the E/Et ratio was comparable with invasive hemodynamic measurements obtained by right heart

catheterization and valuable as a prognostic tool for cardiovascular events in patients with chronic pulmonary artery hypertension [121] (Table 7).

Degree of diastolic dysfunction	Tricuspid E/A ratio	Additional parameters
Impaired relaxation	< 0.8	E/Et >6
Pseudonormal filling	0.8 – 2.1	diastolic flow predominance in the hepatic veins TDE < 120 msec
Restrictive filling	> 2.1	late systolic anterograde flow in the pulmonary artery

Table 7. Right ventricle diastolic dysfunction assessment

c. Clinical Application

As in the case of the left ventricle, RV diastolic function is the first to be impaired, preceding systolic dysfunction. Therefore, when RV impairment is suspected, diastolic function assessment is advised, as RV diastolic dysfunction has been confirmed as a marker of poor prognosis [23]. Most studies support the use of the following parameters: trans-tricuspid E/A ratio, E/E_t ratio, and RA size [23].

4.1.2. Color M-mode flow propagation velocity

a. Acquisition and measurements:

Color M-Mode flow propagation velocity (Vp) is most commonly measured by the slope method from the apical 4-chamber view, using color flow imaging with a narrow color sector; gain is adjusted to avoid noise. The M-mode cursor is placed at the center of the RV inflow blood column from the tricuspid valve to the apex. The color flow baseline is shifted to lower the Nyquist limit so that the central highest velocity jet is blue. Flow propagation velocity (Vp) is measured as the slope of the first aliasing velocity during early filling, measured from the tricuspid valve plane to 4 cm distally into the RV cavity. Alternatively, the slope of the transition from no color to color may be measured.

b. Qualitative values:

Vp values >50 cm/s are considered normal for the RV. The Et/Vp ratio varies proportionally with RA pressure, and may therefore be used either by itself, or in combination with IVRT to assess filling pressures. However, this rather challenging method is redundant in patients with decreased RV ejection fraction in which other parameters precisely identify diastolic dysfunction.

c. Clinical Application

The slowing of tricuspid-to-apical flow propagation measured by color M-mode Doppler is valuable in identifying diastolic dysfunction. In addition, it may help in assessing filling pressures when used in conjunction with tricuspid E. Essays were made to measure non-invasively the tricuspid-to-apical pressure gradient by color M-mode Doppler, but the method

is not currently intended for routine clinical application, due to its difficulty. The non-invasive imaging assessment of the RV has gained raising interest and recent research has provided data which may improve standard clinical protocols. However, highly accurate reference values are yet to be established, and there are currently few available and reproducible parameters.
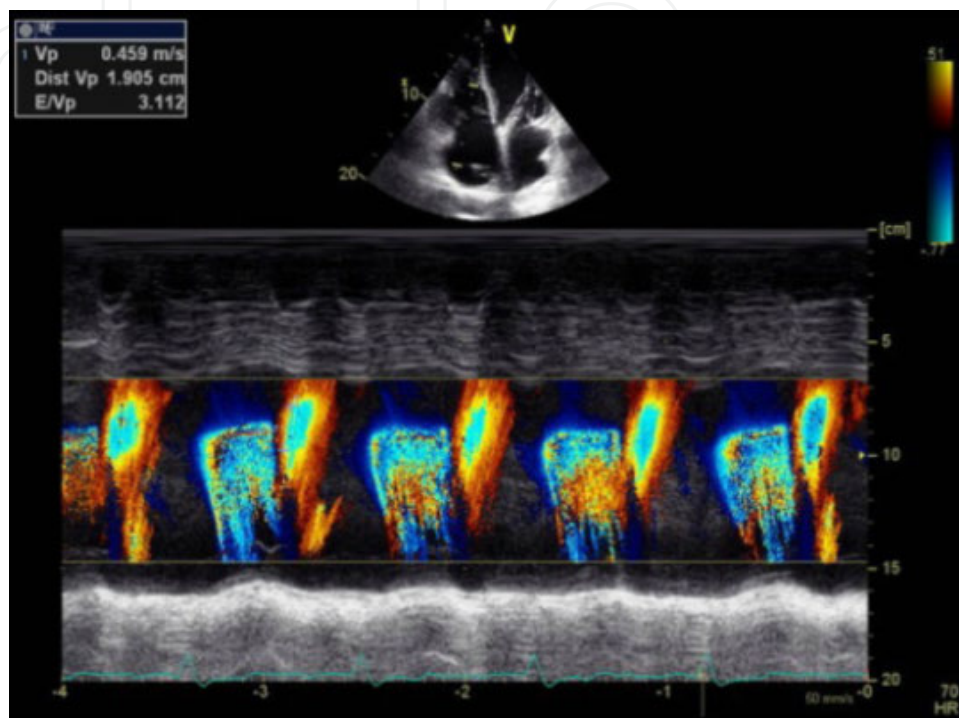

Figure 15. Pulsed color M-mode Vp imaging with the sample placed at the level of the tricuspid annulus of the RV free wall in pulmonary artery hypertension individual.

4.2. Cardiac magnetic resonance imaging

a.   Acquisition and measurements:

The assessment of RV diastolic dysfunction by cardiac MRI is similar, as a principle, to the echocardiographic evaluation. 1.5 Tesla systems can be used to characterize the transtricuspid flow. To this purpose, 4-chamber views should be acquired. ECG-gated phase-contrast pulse sequences are positioned retrospectively, in a plane perpendicular to the transtricuspid inflow, at the level of the opened tricuspid tips, just bellow the tricuspid valve annulus. Two dynamic phase-contrast series, corresponding to an entire cardiac cycle, are acquired during breathhold: 1) the transtricuspid flow velocity sequence, and 2) a myocardial longitudinal velocity sequence. Due to technical progress, cardiac MRI is increasingly being used for blood and myocardial velocities assessment. In addition to that, several studies have demonstrated the usefulness of phase-contrast MRI for measuring diastolic function parameters [122]. However, these analyses are mostly based on manual positioning of regions of interest (ROIs) within the transtricuspid flow area or the myocardium on multiple phases [122, 123]. The derivative of

the time/volume curve, expressed as peak filling rate is used to quantify diastolic function. The early and active peak tricuspid filling rates (PFR_E and PFR_A) and their ratio may be calculated [104].

b. Qualitative values:

Maceira et al [104] published the first normal ranges for MRI-derived RV diastolic function: PFR_E=371 mL/s, or 202 mL/m^2, PFR_A=429 mL/s, or 233 mL/m^2, PFR_E/PFR_E = 0.9 were significantly higher in males [104].

5. Hemodynamic assessment

As previously mentioned, Doppler echocardiography may be used for the non-invasive, indirect assessment of pulmonary artery pressures. To this purpose, the RV-RA pressure gradient is calculated by analyzing the tricuspid regurgitation flow and the obtained value is added to the estimated RA pressure; the latter is estimated by measuring the IVC and its collapsibility after a "sniff". The value of sPAP thusly derived is somewhat empirical. Several studies have shown that Doppler echocardiography systematically under- or overestimates pulmonary pressures, by comparison with direct, invasive measurements by right heart catheterization [96, 124].

Currently, right heart catheterization remains the gold standard for pulmonary artery pressure assessment, as it is necessary to confirm the diagnosis, assess hypertension severity and the reactivity to vasodilator agents [90]. Invasive measurements are particularly useful in patients with NYHA II and III heart failure who have mild pulmonary hypertension as assessed by echocardiography. In addition to that, right heart catheterization provides the advantage of vasoreactivity testing, which is compulsory before initiating vasodilator therapy and may help predict the response to treatment; nitric oxide, adenosine and epoprostenol are most commonly used for this purpose [90]. Patients who have an acute response to vasoreactivity testing are more likely to respond to long-tem therapy [125].

In conclusion, echocardiography may be used as a screening method, as it indicates the likelihood of pulmonary artery hypertension, rather than providing an actual diagnosis. Results should always be validated by right heart catheterization, particularly if specific vasodilator treatment is intended. All in all, 2D echocardiography has some limitations, some related to the empirical assessment of sPAP, others to the imprecision in chamber measurements due to geometrical assumptions or difficult endocardial border tracing. Presently, cardiac MRI is the golden standard in RV structure and function evaluation, due to its unlimited imaging planes, higher image resolution, and the ability to calculate volumes using three-dimensional measurements; however, cardiac MRI is seldom available in many centres, and hindered by prolonged acquisition and processing times. Moreover, its use is still limited in patients with implanted metallic devices, such as pace-makers, defibrillators, metallic prostheses or insulin pumps. Right heart catheterization allows a good evaluation of sPAP, but it is an invasive procedure and is not usually performed in the absence of other evidence

of pulmonary artery hypertension. Standard 2D echocardiography is widely available, relatively cheap, does not present any risk for the patient, and may be performed even in the presence of metallic devices which would normally hinder an MRI examination. Although it only indicates the likelihood of pulmonary artery hypertension, it may be used to select candidates for right catheterization. In terms of assessing RV structure and function, further research would be needed in order to provide solid, reproducible parameters, with normal reference values.

Acknowledgements

Author details

Lucia Agoston-Coldea[1] and Silvia Lupu[2]

*Address all correspondence to: luciacoldea@yahoo.com

1 The "Iuliu Hatieganu" University of Medicine and Pharmacy, Cluj-Napoca, Romania

2 The University of Medicine and Pharmacy of Targu Mures, Romania

References

[1] Kasimir, M.T, Seebacher, G, Jaksch, P, Winkler, G, Schmid, K, Marta, GM, Simon, P, & Klepetko, W. Reverse cardiac remodelling in patients with primary pulmonary hypertension after isolated lung transplantation. Eur J Cardiothorac Surg. (2004)., 26(4), 776-781.

[2] McLaughlin, V.V, Archer, S.L, Badesch, D.B, Archer, S.L, Badesch, D.B, Barst, R.J, Farber, H.W, Lindner, J.R, Mathier, M.A, McGoon, M.D, Park, M.H, Rosenson, R.S, Rubin, L.J, Tapson, V.F, & Varga, J. ACCF/AHA 2009 expert consensus document on pulmonary hypertension. J Am Coll Cardiol. (2009)., 53(17), 1573-1619.

[3] Badano, L.P, Ginghina, C, Easaw, J, Muraru, D, Grillo, M.T, Lancellotti, P, Pinamonti, B, Coghlan, G, Marra, M.P, Popescu, B.A, & De Vita, S. Right ventricle in pulmonary arterial hypertension: hemodynamics, structural changes, imaging and proposal of a study protocol aimed to assess remodelling and treatment effects. Eur J Echocardiogr. (2010)., 11(1), 27-37.

[4] Grapsa, J, O'Regan, D.P, Pavlopoulos, H, Durighel, G, Dawson, D, & Nihoyannopoulos, P. Right ventricular remodelling in pulmonary arterial hypertension with three-dimensional echocardiography: comparison with cardiac magnetic resonance imaging. Eur J Echocardiogr. (2010)., 11(1), 64-73.

[5] Kostrubiec, M, Kaczynska, A, & Pruszczyk, P. Right ventricle remodelling and elevated D-dimer concentration in patients 6 months after first episode of acute pulmonary embolism. Eur Heart J. (2008)., 29(16), 2059-2060.

[6] Mansi, T, Voigt, I, Leonardi, B, Pennec, X, Durrleman, S, Sermesant, M, Delingette, H, Taylor, A.M, Boudjemline, Y, Pongiglione, G, & Ayache, N. A statistical model for quantification and prediction of cardiac remodelling: application to tetralogy of Fallot. IEEE Trans Med Imaging. (2011)., 30(9), 1605-1616.

[7] Haddad, F, Doyle, R, Murphy, D.J, & Hunt, S.A. Right Ventricular Function in Cardiovascular Disease, Part II: Pathophysiology, Clinical Importance, and Management of Right Ventricular Failure. Circulation. (2008)., 117(13), 1717-1731.

[8] Haddad, F, Hunt, S.A, Rosenthal, D.N, & Murphy, D.J. Right Ventricular Function in Cardiovascular Disease, Part I: Anatomy, physiology, aging, and functional assessment of right ventricle. Circulation. (2008)., 117(11), 1436-1448.

[9] Haddad, F, Couture, P, Tousignant, C, & Denault, A.Y. The right ventricle in cardiac surgery, a perioperative perspective: I. Anatomy, Physiology, and Assessment. Anesth Analg. (2009)., 108(2), 407-421.

[10] Valsangiacomo Buechel, E.R, & Mertens, L.L. Imaging the right heart: the use of integrated multimodality imaging. Eur Heart J. (2012)., 33(8), 949-960.

[11] Niemann, P.S, Pinho, L, Balbach, T, Galuschky, C, Blankenhagen, M, Silberbach, M, Broberg, C, Jerosch-Herold, M, & Sahn, D.J. Anatomically oriented right ventricular volume measurements with dynamic three-dimensional echocardiography validated by 3-Tesla magnetic resonance imaging. J Am Coll Cardiol. (2007)., 50(17), 1668-1676.

[12] Martin, E.T, Coman, J.A, Shellock, F.G, Pulling, C.C, Fair, R, & Jenkins, K. Magnetic resonance imaging and cardiac pacemaker safety at 1.5-Tesla. J Am Coll Cardiol. (2004)., 43(7), 1315-1324.

[13] Juntilla, M.J, Fishman, J.E, Loperal, G.A, Pattany, P.M, Velasquez, D.L, Williams, A.R, Trachtenberg, B.H, Sanina, C, Mather, J, & Hare, J.M. Safety of serial MRI in patients with implantable cardioverter defibrillators. Heart. (2011)., 97(22), 1852-1856.

[14] Naehle, C.P, Strach, K, Thomas, D, Meyer, C, Linhart, M, Bitaraf, S, Litt ,H, Schwab, J.O, Schild, H, & Sommer, T. Magnetic Resonance Imaging at 1.5-T In Patients With Implanted Cardioverter Defibrillators. J Am Coll Cardiol. (2009)., 54(6), 549-555.

[15] Rosenthal, D, Chrisant, M.R, Edens, E, Mahony, L, Canter, C, Colan, S, Dubin, A, Lamour, J, Ross, R, Shaddy, R, Addonizio, L, Beerman, L, Berger, S, Bernstein, D, Blume, E, Boucek, M, Checchia, P, Dipchand, A, Drummond-Webb, J, Fricker, J,

Friedman, R, Hallowell, S, Jaquiss, R, Mital, S, Pahl, E, Pearce, F.B, Rhodes, L, Rotondo, K, Rusconi, P, Scheel, J, Pal Singh, T, & Towbin, J. International Society for Heart and Lung Transplantation: Practice guidelines for management of heart failure in children. J Heart Lung Transplant. (2004)., 23(12), 1313-1333.

[16] Crean, A, Ballard, G, Maredia, N, Greenwood, J.P, & Thomson, J.D. 3D echo systematically underestimates right ventricular volume compared to cardiac magnetic resonance in adult congenital heart disease patients with moderate or severe RV dilatation. J Cardiovasc Magn Reson. (2011)., 13, 78.

[17] van der Zwaan, H.B, Helbing, W.A, McGhie, J.S, Geleijnse, M.L, Luijnenburg, S,E, Roos-Hesselink, J.W, & Meijboom, F.J. Clinical value of real-time three-dimensional echocardiography for right ventricular quantification in congenital heart disease: validation with cardiac magnetic resonance imaging. J Am Soc Echocardiogr. (2010)., 23(2), 134-140.

[18] Ho, S.Y, & Nihoyannopoulos, P. Anatomy, echocardiography, and normal right ventricular dimensions. Heart. (2006)., 92 (suppl 1), i2-13.

[19] Chen, P.S, Moser, K.M, Dembitsky, W.P, Auger, W.R, Daily, P.O, Calisi, C.M, Jamieson S.W, & Feld, G.K. Epicardial activation and repolarization patterns in patients with right ventricular hypertrophy. Circulation. (1991)., 83(1), 104-118.

[20] Bashore TM. Adult congenital heart disease: right ventricular outflow tract lesions. Circulation. (2007)., 115(14), 1933-1947.

[21] Arya, A, Piorkowski, C, Sommer, P, Gerds-Li, J.H, Kottkamp, H, & Hindricks, G. Idiopathic outflow tract tachycardia: current perspectives. Herz. (2007)., 32(3), 218-225.

[22] Yoerger, D.M, Marcus, F, Sherill, D, Calkins, H, Towbin, J.A, Zareba, W, Picard, M.H. Echocardiographic findings in patients meeting task force criteria for arrhythmogenic right ventricular dysplasia: new insights from the multidisciplinary task study of right ventricular dysplasia. J Am Coll Cardiol. (2005)., 45(6), 860-865.

[23] Rudski, L.G, Lai, W.W, Afilalo, J, Hua, L, Handschumacher, M.D, Chandrasekaran, K, Solomon, S.D, Louie, E.K, & Schiller, N.B. Guidelines for the Echocardiographic Assessment of the Right Heart in adults: A Report fron the American Society of Echocardiography, a registered branch of the European Society of Cardiology, and the Canadian Society of Echocardiography. J Am Soc Echocardiogr. (2010)., 23(7), 685-713.

[24] Mor-Avi, V, Lang, R.M, Badano, L.P, Belohlavek, M, Cardim, N.M, Derumeaux, G, Galderisi, M, Marwick, T, Nagueh, SF, Sengupta, P.P, Sicari, R, Smiseth, O.A, Takeuchi M, Thomas, J.D, Vannan, M, Voigt, J.U, & Zamorano, J.L. Current and Evolving Echocardiographic Techniques for the Quantitative Examination of Cardiac Mechanics: ASE/EAE Consensus Statement on Methodology and Indications Endorsed by the Japanese Society of Echocardiography. Eur J Echocardiogr. (2011)., 12(3), 167-205.

[25] Brittain, E.L, Hemnes, A.R, Keebler, M, Lawson, M, Byrd, B.F, & DiSalvo, T. Right ventricular plasticity and functional imaging. Pulm Circ. (2012)., 2(3), 309-326.

[26] Grapsa, J, Dawson, D, & Nihoyannopoulos, P. Assessment of Right Ventricular Structure and Function in Pulmonary Hypertension. J Cardiovasc Ultrasound. (2011)., 19(3), 115-125.

[27] Feigenbaum, H, Armstrong, W, & Ryan, T. Left atrium, right atrium, right ventricle. In: Feigenbaum H (ed.) Feigenbaum's echocardiography. 6th ed. Philadelphia: Lippincot, Williams and Wilkins. (2005)., 181-213.

[28] Ryan, T, Petrovic, O, Dillon, J.C, Feigenbaum, H, Conley, M.J, & Armstrong, WF. An Echocardiographic Index for Separation of Right Ventricular Volume and Pressure Onverload. J Am Coll Cardiol. (1985)., 5(4), 918-924.

[29] López-Candales, A, Rajagopalan, N, Kochar, M, Gulyasy, B, & Edelman, K. Systolic eccentricity index identifies right ventricular dysfunction in pulmonary hypertension. Int J Cardiol. (2008)., 129(3), 424-426.

[30] Lang, R.M, Bierig, M, Devereux, R.B, Flachskampf, F.A, Foster, E, Pellikka, P.A, Picard, M.H, Roman, M.J, Seward, J, Shanewise, J.S, Solomon, S.D, Spencer, K.T, Sutton, M.S, & Stewart, W.J. Recommendations for chamber quantification: a report from the American Society of Echocardiography's Guidelines and Standards Committee and the Chamber Quantification Writing Group, developed in conjunction with the European Association of Echocardiography, a branch of the European Society of Cardiology. J Am Soc Echocardiogr. (2005)., 18(12), 1440-1463.

[31] Kovalova, S, Necas, J, & Vespalec, J. What is a "normal" right ventricle? Eur J Echocardiogr. (2006)., 7(4), 293-297.

[32] Gillam, L.D, & Otto, C.M. Advanced Approaches in Echocardiography. Philadelphia: Elsevier Inc. Saunders. (2012).

[33] Tamborini, G, Marsan, N.A, Gripari, P, Maffessanti Brusoni, D, Muratori, M, Caiani, E.G, Fiorentini, C, & Pepi, M. Reference values for right ventricular volumes and ejection fraction with real-time three-dimensional echocardiography: evaluation in a large series of normal subjects. J Am Soc Echocardiogr. (2010)., 23(2), 116-126.

[34] Gopal, A.S, Chukwu, E.O, Iwuchukwu, C.J, Katz, A.S, Toole, R.S, Schapiro, W, & Reichek, N. Normal Values of Right Ventricular Size and Function by Real-time 3-Dimensional Echocardiography: Comparison with Cardiac Magnetic Resonance Imaging. J Am Soc Echocardiogr. (2007)., 20(5), 445-455.

[35] Lopez-Candales, A, Dohi, K, Rajagopalan, N, Edelman, K, Gulysasy, B, & Bazaz, R. Defining normal variables of right ventricular size and function in pulmonary hypertension: an echocardiographic study. Postgrad Med J. (2008)., 84(987), 40-45.

[36] Lopez-Candales, A, Bazaz, R, Edelman, K, & Gulyasy, B. Apical Systolic Eccentricity Index: A Better Marker of Right Ventricular Compromise in Pulmonary Hypertension. Echocardiogr. (2010)., 27(5), 534-538.

[37] Frances RJ. Arrhythmogenic right ventricle dysplasia/cardiomyopathy. A review and update. Int J Cardiol. (2006)., 110(3), 279-287.

[38] Muller, H, Noble, S, Keller, P.F, Sigaud, P, Gentil, P, Lerch, R, Shah, D, & Burri, H. Biatrial anatomical reverse remodeling after radiofrequency catheter ablation for atrial fibrillation: evidence from real-time three-dimensional echocardiography. Europace. (2008)., 10(9), 1073-1078.

[39] Wang, Y, Gutman, J.M, Heilbron, D, Wahr, D, & Schiller, NB. Atrial volume in a normal adult population by two-dimensional echocardiography. Chest. (1984)., 86(4), 595-601.

[40] Quraini, D, Pandian, N.G, & Patel, A.R. Three-dimensional echocardiographic analysis of right atrial volume in normal and abnormal hearts: comparison of biplane and multiplane methods. Echocardiogr. (2012)., 29(5), 608-613.

[41] Faletra, F.F, Ho, S.Y, & Auricchio, A. Anatomy of Right Atrial Structures by Real-Time 3D Transesophageal Echocardiography. JACC Cardiovasc Imaging. (2010)., 3(9), 966-975.

[42] Aune, E, Baekkevar, M, Roislien, J, Rodevand, O, & Otterstad, J.E. Normal reference ranges for left and right atrial volume indexes and ejection fractions obtained with real-time three-dimensional echocardiography. Eur J Echocardiogr. (2009)., 10(6), 738-744.

[43] Jardin, F, & Vieillard-Baron, A. Ultrasonographic examination of the venae cavae. Intense Care Med. (2006)., 32(2), 203-206.

[44] Otto CM. Textbook of clinical Echocardiography. 3rd Edition. Philadelphia: Elsevier Saunders. (2004)., 154-159.

[45] Brierre, G, Blot-Souletie, N, Degano, B, Tetu, L, Bongard, V, & Carrie, D. New echocardiographic prognostic factors for mortality in pulmonary arterial hypertension. Eur J Echocardiogr. (2010)., 11(6), 516-522.

[46] Hudsmith, L.E, Petersen, S.E, Francis, J.M, Robson, M.D, & Neubauer, S. Normal human left and right ventricular and left atrial dimensions using steady state free precession magnetic resonance imaging.J Cardiovasc Magn Reson. (2005)., 7(5), 775-782.

[47] Shiota T. 3D echocardiography: evaluation of the right ventricle. Curr Opin Cardiol. (2009)., 24(5), 410-414.

[48] Sugeng, L, Mor-Avi, V, Weinert, L, Niel, J, Ebner, C, Steringer-Mascherbauer, R, Bartolles, R, Baumann, R, Schummers, G, Lang, R.M, & Nesser, H.J. Multimodality Com-

parison of Quantitative Volumetric Analysis of the Right Ventricle. JACC Cardiovasc Imaging. (2010)., 3(1), 10-18.

[49] Raymond, R.J, Hinderliter, A.L, Willis, P.W, Ralph, D, Caldwell, E.J, Williams, W, Et-tinger, N.A, Hill, N.S, Summer, W.R, De Boisblanc, B, Schwartz, T, Koch, G, Clayton, L.M, Jobsis, M.M, Crow, J.W, & Long, W. Echocardiographic predictors of adverse outcomes in primary pulmonary hypertension. J Am Coll Cardiol. (2002)., 39(7), 1214-1219.

[50] Anavekar, N.S, Skali, H, Bourgoun, M, Ghali, J.K, Kober, L, Maggioni, A.P, McMur-ray, J.J, Velazquez, E, Califf, R, Pfeffer, M.A, & Solomon, S.D. Usefulness of right ven-tricular fractional area change to predict death, heart failure, and stroke following myocardial infarction (from the VALIANT ECHO study). Am J Cardiol. (2008)., 101(5), 607-612.

[51] Meluzin, J, Spinarova, L, Hude, P, Krejci, J, Kincl, V, Panovsky, R, & Dusek, L. Prog-nostic importance of various echocardiographic right ventricle functional parameters in patients with symptomatic heart failure. J Am Soc Echocardiogr. (2005)., 18(5), 435-444.

[52] Ghio, S, Gavazzi, A, Campana, C, Inserra, C, Klersy, C, Sebastiani, R, Arbustini, E, Recusani, F, & Tavazzi L. Independent and additive prognostic value of right ven-tricular systolic function and pulmonary artery pressure in patients with chronic heart failure. J Am Coll Cardiol. (2001)., 37(1), 183-188.

[53] Zimbarra Cabrita, I, Ruisanchez, C, Dawson, D, Grapsa, J, North, B, Howard, L.S, Pinto, F.J, Nihoyannopoulos, P, & Gibbs, J.R.S. Right ventricular function in patients with pulmonary hypertension; the value of myocardial performance index measured by tissue Doppler imaging. Eur J Echocardiogr. (2010)., 11(8), 719-724.

[54] Miller, D, Farah, M.G, Liner, A, Fox, K, Schluchter, M, & Hoit, B.D. The relation be-tween quantitative right ventricular ejection fraction and indices of tricuspid annular motion and myocardial perfromance. J Am Soc Echocardiogr. (2004)., 17(5), 443-447.

[55] Forfia, P.R, Fisher, M.R, Mathai, S.C, Housten-Harris, T, Hemnes, A.R, Borlaug, B.A, Chamera, E, Corretti, E, Champion, H.C, Abraham, T.P, Girgis R.E, & Hassoun, P.M. Tricuspid annular displacement predicts survival in pulmonary hypertension. Am J Respir Crit Care Med. (2006)., 174(9), 1034-1041.

[56] Kaul, S, Tei, C, Hopkins, J.M, & Shah, P.M. Assessment of right ventricular function using two-dimensional echocardiography. Am Heart J. (1984)., 107(3), 526-531.

[57] Lindqvist, P, Waldenstrom, A, Henein, M, Morner, S, & Kazzam, E. Regional and global right ventricular function in normal individuals aged 20-90 years: a pulsed Doppler tissue imaging study: Umea General Population Heart Study. Echocardiogr. (2005)., 22(4), 305-314.

[58] Lindqvist, P, Waldenstrom, A, Wikstrom, G, & Kazzam, E. The use of isovolumic contraction velocity to determine right ventricular state of contractility and filling

pressures: A pulsed Doppler tissue imaging study. Eur J Echocardiogr. (2005)., 6(4), 264-270.

[59] Kukulski, N.P, Hubbert, L, Arnold, M, Wranne, B, Hatle, L, & Sutherland, G.R. Normal regional right ventricular function and its change with age: a Doppler myocardial imaging study. J Am Soc Echocardiogr. (2000)., 13(3), 194-204.

[60] Bleeker, G.B, Steendijk, P, Holman, E.R, Yu, C.M, Breitharth, O.A, Kaandorp, T.A.M, Schalij, M.J, van der Wall, E.E, Nihoyannopoulos, P, & Bax, J.J. Assessing right ventricular function: the role of echocardiography and complementary technologies. Heart. (2006)., 92(Suppl 1), i19–i26.

[61] Vogel, M, Schmidt, M.R, Kristiansen, S.B, Cheung, M, White, P.A, Sorensen, K, & Redington, A.N. Validation of myocardial acceleration during isovolumic contraction as a novel noninvasive index of right ventricular contractility: comparison with ventricular pressure-volume relations in an animal model. Circulation. (2002)., 105(14), 1693-1699.

[62] Hashimoto, I, Li, X.K, Hejmadi Bhat, A, Jones, M, & Sahn, D.J. Quantitative assessment of regional peak myocardial acceleration during isovolumic contraction and relaxation time by tissue Doppler imaging. Heart. (2005)., 91(6), 811-816.

[63] Tayyareci, Y, Tayyareci, G, Tastan, C.P, Bayazit, P, & Nisanci, Y. Early diagnosis of right ventricular systolic dysfunction by tissue Doppler-derived isovolumic myocardial acceleration in patients with chronic obstructive pulmonary disease. Echocardiogr. (2009)., 26(9), 1026-1035.

[64] Tugcu, A, Yildirimturk, O, Tayyareci, Y, Demiroglu, C, & Aytekin, S. Evaluation of subclinical right ventricular dysfunction in obstructive sleep apnea patients using velocity vector imaging. Circ J. (2010)., 74(2), 312-319.

[65] Tayyareci, Y, Yurdakul, S, Tayyareci, G, Nisanci, Y, Umman, B, & Bugra, Z. Impact of myocardial acceleration during isovolumic contraction in evaluating subclinical right ventricular systolic dysfunction in type 2 diabetes mellitus patients. Echocardiogr. (2010)., 27(10), 1211-1218.

[66] Tayyareci, Y, Nisanci, Y, Umman, B, Oncul, A, Yurdakul, S, Altun, I, Umman, S, & Bugra, Z. Early detection of right ventricular systolic dysfunction by using myocardial acceleration during isovolumic contraction in patients with mitral stenosis. Eur J Echocardiogr. (2008)., 9(4), 516-521.

[67] Schattke, S, Knebel, F, Grohmann, A, Dreger, H, Kmezik, F, Riemekasten, G, Baumann, G, & Borges, A.C. Early right ventricular systolic dysfunction in patients with systemic sclerosis without pulmonary hypertension: a Doppler Tissue and Speckle Tracking echocardiography study. Cardiovasc Ultrasound. (2010)., 8, 3.

[68] Arnold, R, Gorenflo, M, Böttler, P, Eichhorn, J, Jung, C, & Goebel, B. Tissue Doppler derived isovolumic acceleration in patients after atrial repair for dextrotransposition of the great arteries. Echocardiogr. (2008)., 25(7), 732-738.

[69] Nikitin, N.P, Loh, P.H, De Silva, R, Witte, K.K, Lukaschuk, E.I, Parker, A, Farnsworth, T.A, Alamgir, F.M, Clark, A.L, & Cleland, J.G. Left ventricular morphology, global and longitudinal function in normal older individuals: a cardiac magnetic resonance study. Int J Cardiol. (2006)., 108(1), 76-83.

[70] Dalen, H, Thorstensen, A, Vatten, L.J, Aase, S.A, & Stoylen, A. Reference Values and Distribution of Conventional Echocardiographic Doppler Measures and Longitudinal Tissue Doppler Velocities in a Population Free From Cardiovascular Disease. Circ Cardiovasc Imaging. (2010)., 3(5), 614-622.

[71] Meluzin, J, Spinarova, L, Bakala, J, Toman, J, Hude, P, Kara, T, & Soucek, M. Pulsed Doppler tissue imaging of the velocity of tricuspid annular systolic motion. A new, rapid, and non-invasive method of evaluating right ventricular systolic function. Eur Heart J. (2001)., 22(4), 340-348.

[72] Lopez-Candales, A, Dohi, K, Bazaz, R, & Edelman, K. Relation of right ventricular free wall mechanical delay to right ventricular dysfunction as determined by tissue Doppler imaging. Am J Cardiol. (2005)., 96(4), 602-606.

[73] Rojo, E.C, Rodrigo, J.L, Perez de Isla, R, Almeria, C, Gonzalo, N, Aubele, A, Cinza, R, Zamorano, J, & Macaya, C. Disagreement between tissue Doppler imaging and conventional pulsed wave Doppler in the measurement of myocardial performance index. Eur J Echocardiogr. (2006)., 7(5), 356-364.

[74] Gaibazzi, N, Petrucci, N, & Ziacchi, V. Left ventricle myocardial performance index derived either by conventional method or mitral annulus tissue Doppler: a comparison study in healthy subjects and subjects with heart failure. J Am Soc Echocardiogr. (2005)., 18(12), 1270-1276.

[75] Duzenli, M.A, Ozdemir, K, Aygul, N, Soylu, A, Aygul, M.U, & Gok, H. Comparison of myocardial performance index obtained either by conventional echocardiography or tissue Doppler echocardiography in healthy subjects and patients with heart failure. Heart Vessels. (2009)., 24(1), 8-15.

[76] Abd El Rahman, M.Y, Hui, W, Dsebissowa, F, Schubert, S, Hubler, M, Hetzer, R, Lange, P.E, & Abdul-Kahliq, H. Comparison of the tissue Doppler-derived left ventricular Tei index to than obtained by Doppler in patients with congenital and acquired hear disease. Pediatr Cardiol. (2005)., 26(4),391-395.

[77] Chockalingam, A, Gnanavelu, G, Alagesan, R, & Subramaniam, T. Myocardial performance index in evaluation of acute right ventricular myocardial infarction. Echocardiogr. (2004)., 21(6), 487-494.

[78] Blanchard, D.G, Malouf, P.J, Gurudevan, S.V, Auger, V.R, Madani, M.M, Thistlethwhite, P, Waltman, T.J, Daniels, L.B, Raisinghani, A.B, DeMaria, A.N. Utility of right

ventricular Tei indexin the noninvasive evaluation of chronic thromboembolic pulmonary hypertension before and after pulmonary thromboendarterectomy. JACC Cardiovasc Imaging. (2009)., 2(2),143-149.

[79] Hsiao, S.H, Lee, C.Y, Chang, S.M, Yang, S.H, Lin, S.K, & Huang, W.C. Pulmonary embolism and right heart function: insights from myocardial Doppler tissue imaging. J Am Soc Echocardiogr. (2006)., 19(6), 822-828.

[80] Hsiao, S.H, Yang, S.H, Wang, W.C, Lee, C.Y, Lin, S.K, & Liu, C.P. Usefulness of regional myocardial performance index to diagnose pulmonary embolism in patients with echocardiographic signs of pulmonary hypertension. Am J Cardiol. (2006)., 98(12), 1652-1655.

[81] Park, J.H, Park, Y.S, Park, S.J, Lee, J.H, Choi, S.W, Jeong, J.O, & Seong, I.W. Midventricular peak systolic strain and Tei index of the right ventricle correlated with decreased right ventricular systolic function in patients with acute pulmonary thromboembolism. Int J Cardiol. (2006)., 125(3), 319-324.

[82] Haddad, F, Denault, A.Y, Couture, P, Cartier, R, Pellerin, M, Levesque, S, Lambert, J, & Tardif, J.C. Right ventricular myocardial performance index predicts perioperative mortality or circulatory failure in high-risk valvular surgery. J Am Soc Echocardiogr. (2007)., 20(9), 1065-1072.

[83] Ishii, M, Eto, G, Tei, C, Tsutsumi, T, Hashino, K, Sugahara, Y, Himeno, W, Muta, H, Furui, J, Akagi, T, Fukiyama, R, Toyoda, O, & Kato, H. Quantitation of the global right ventricular function in children with normal heart and congenital heart disease: a right ventricular myocardial performance index. Pediatr Cardiol. (2000)., 21(5), 416-421.

[84] Eidem, B.W, Tei, C, O'Leary, P.W, Cetta, F, & Seward, J.B. No geometric quantitative assessment of right and left ventricular function: Myocardial performance index in normal children and patients with Ebstein anomaly. J Am Soc Echocardiogr. (1998)., 11(9), 849-856.

[85] Romero-Corral, A, Somers, V.K, Pellikka, P.A, Olson, E.J, Bailey, K.R, Korinek, J, Orban, M, Sierra-Johnson, J, Kato, M, Amin, R.S, & Lopez-Jimenez, F. Decreased Right and Left Ventricular Myocardial Performance in Obstructive Sleep Apnea. Chest. (2007)., 132(6), 1863-1870.

[86] Jurcut, R, Giusca, S, La Gerche, A, Vasile, S, Ginghina, C, & Voigt, J.U. The echocardiographic assessment of the right ventricle: what to do in 2010? Eur J Echocardiogr. (2010)., 11(2), 81-96.

[87] Brecker, S.J.D, Gibbs, J.S.G, Fox, K.M, Yacoub, M.H, & Gibson, D.G. Comparison of Doppler derived haemodynamic variables and simultaneous high fidelity pressure measurements in severe pulmonary hypertension. Br Heart J. (1994)., 72(4), 384-389.

[88] Anconina, J, Danchin, N, Selton-Suty, C, Isaaz, K, Juilliere, Y, Buffet, P, Edel, F, & Cherrier, F. Measurement of right ventricular dp/dt. A simultaneous/comparative he-

modynamic and Doppler echocardiographic study. Arch Mal Coeur Vaiss. (1992)., 85(9), 1317-1321.

[89] Kanzaki, H, Nakatani, S, Kawada, T, Yamagishi, M, Sunagawa, K, & Miyatake, K. Right ventricular dP/dt/P(max), not dP/dt(max), noninvasively derived from tricuspid regurgitation velocity is a useful index of right ventricular contractility. J Am Soc Echocardiogr. (2002)., 15(2), 136-142.

[90] Galie, N, Hoeper, M.M, Humbert, M, Torbicki, A, Vachiery, J.L, Barbera, J.A, Beghetti, M, Corris, P, Gaine, S, Gibbs, J.S, Gomes-Sanchez, M.A, Jondeau, G, Klepetko, W, Opitz, C, Rubin, L, Zellweger, M, & Simonneau, G. Guidelines for the diagnostis and treatment of pulmonary artery hypertension. Eur Heart J. (2009)., 30(20), 2493-2537.

[91] Habib, G, & Torbiki, A. The role of echocardiography in the diagnosis and management of patients with pulmonary hypertension. Eur Respir Rev. (2010)., 19(118), 288-299.

[92] Abraham, J, & Abraham, T.P. The Role of Echocardiography in Hemodinamic Assessment in Heart failure. Heart Fail Clin. (2009)., 5(2), 191-208.

[93] Ristow, B, & Schiller, N.B. Stepping away from ritual right heart catheterisation into the era of non-invasively measured pulmonary artery pressure. J Am Soc Echocardiogr. (2009)., 22(7), 820-822.

[94] Milan, A, Magnino, C, & Veglio, C. Echocardiographic indexes for the non-invasive evaluation of pulmonary hemodynamics. J Am Soc Echocardiogr. (2010)., 23(3), 225-239.

[95] Dabestani, A, Mahan, G, Gardin, JM, Takenaka, K, Burn, C, Allfie, A, & Henry, W.L. Evaluation of the pulmonary artery pressure and resistance by Doppler echocardiography. Am J Cardiol. (1987)., 59 (6), 662-668.

[96] Fisher, M.R, Forfia, F.R, Chamera, E, Housten-Harris, T, Champion, H.C, Girgis, R.E, Corretti, M.C, & Hassoun, P.M. Accuracy of Echocardiography in the hemodynamic assessment of pulmonary hypertension. Am J Respir Crit Care Med. (2009)., 179(7), 615-621.

[97] McGoon, M, Gutterman, D, Steen, V, Barst, R, McCrory, D.C, Fortin, T.A, & Loyd, J.E. Screening, early detection and diagnosis of pulmonary arterial hypertension: ACCP evidence-based clinical practice guidelines. Chest. (2004)., 126(suppl 1), 14S-34S.

[98] Ozdemir, K, Altunkeser, B.B, Icli, A, Ozdil, H, & Gok, H. New Parameters in identification of right ventricle myocardial infarction and proximal right coronary artery lesion. Chest. (2003)., 124(1), 219-226.

[99] Kowalski, M, Kukulski, T, Jamal, F, D'hooge, J, Weidemann, F, Rademakers, F, Bijnens, B, Hatle, L, & Sutherland, G.R. Can natural strain and strain rate quantify re-

gional myocardial deformation? A study in healthy subjects. Ultrasound Med Biol. (2001)., 27(8), 1087-1097.

[100] Marwick TH. Measurement of strain and strain rate by echocardiography: ready for prime time? J Am Coll Cardiol. (2006)., 47(7), 1313-1327.

[101] Teske, A.J, De Boeck, B.W, Olimulder, M, Prakken, N.H, Doevendans, P.A, & Cramer, M.J. Echocardiographic assessment of regional right ventricular function: a head-to-head comparison between 2-dimensional and tissue Doppler-derived strain analysis. J Am Soc Echocardiogr. (2008)., 21(3), 275-283.

[102] Cho, E.J, Jiamsripong, P, Calleja, A.M, Alharthi, M.S, McMahon, E.M, Khandheria, B.K, & Belohlavek, M. Right ventricular free wall circumferential strain reflects graded elevation in acute right ventricular afterload. Am J Physiol Heart Circ Physi. (2009)., 296(2), H413-H420.

[103] Benza, R, Biederman, R, Murali, S, & Gupta, H. Role of cardiac magnetic resonance imaging in the management of patients with pulmonary arterial hypertension. J Am Coll Cardiol. 2008; 52(21):1683-1692.

[104] Maceira, A.M, Prasad, S.K, Khan, M, & Pennell, D.J. Reference right ventricular systolic and diastolic function normalized to age, gender and body surface area from steady-state free precession cardiovascular magnetic resonance. Eur Heart J. (2006)., 27(23), 2879-2888.

[105] Leibundgut, G, Rohner, A, Grize, L, Bernheim, A, Kessel-Schaefer, A, Bremerich, J, Zellweger, M, Buser, P, & Handke, M. Dynamic Assessment of Right Ventricular Volumes and Function by Real-Time Three-Dimensional Echocardiography: A Comparison Study With Magnetic Resonance Imaging in 100 Adult Patients. J Am Soc Echocardiogr. (2010)., 23(2), 116-126.

[106] Lu, X, Nadvoretskiy, V, Bu, L, Stolpen, A, Ayres, N, Pignatelli, R.H, Kovalchin, J.P, Grenier, M, Klas, B, & Ge, S. Accuracy and reproducibility of real-time three-dimensional echocardiography for assessment of right ventricular volumes and ejection fraction in children. J Am Soc Echocardiogr. (2008)., 21(1), 84-89.

[107] Kjaergaard, J, Petersen, C.L, Kjaer, A, Schaadt, BK, Oh, J.K, & Hassager, C. Evaluation of right ventricular volume and function by 2D and 3D echocardiography compared to MRI. Eur J Echocardiogr. (2006)., 7(6), 430-438.

[108] Vonk-Noordegraaf, A, Marcus, J.T, Gan, C.T, Boonstra, A, & Postmus, P.E. Interventricular mechanical asynchrony due to right ventricular pres-sure overload in pulmonary hypertension plays an important role in impaired left ventricular filling. Chest. (2005)., 128(Suppl 6), 628S–630S.

[109] Crean, A.M, Maredia, N, Ballard, G, Menezes, R, Wharton, G, Forster, J, Greenwood, J.P, & Thomson, J.D. 3D Echo systematically underestimates right ventricular volumes compared to cardiovascular magnetic resonance in adult congenital heart dis-

ease patients with moderate or severe RV dilatation. J Cardiovasc Magn Reson. (2011)., 13, 78.

[110] Wang, J, Prakasa, K, Bomma, C, Tandri, H, Dalal, D, James, C, Tichnell, C, Corretti, M, Bluemke, D, Calkins, H, & Abraham, T.P. Comparison of novel echocardiographic parameters of right ventricular function with ejection fraction by cardiac magnetic resonance. J Am Soc Echocardiogr. (2007)., 20(9), 1058-1064.

[111] Pavlicek, M, Wahl, A, Rutz, T, De Marchi, S.F, Hille, R, Wustmann, K, Steck, H, Eigenmann, C, Schwerzmann, M, & Seiler, C. Right ventricular systolic function assessment: rank of echocardiographic methods vs. cardiac magnetic resonance imaging. Eur J Echocardiogr. (2011)., 12(11), 871-880.

[112] Klein, A.L, Leung, D.Y, Murray, R.D, Urban, L.H, Bailey, K.R, & Tajik, A.J. Effects of age and physiologic variables on right ventricular filling dynamics in normal subjects. Am J Cardiol. (1999)., 84(4), 440-448.

[113] Berman, J.L, Green, L.H, & Grossman, W. Right ventricular diastolic pressure in coronary artery disease. Chest. (1979)., 44(7), 1263-1268.

[114] Marwick TH. Clinical application of tissue Doppler imaging: a promise fulfilled. Heart. (2003)., 89(12), 1377-1378.

[115] Pellerin, D, Sharma, R, Elliot, P, & Veyrat, C. Tissue Doppler, strain, and strain rate echocardiography for the assessment of left and right systolic ventricular function. Heart. (2003)., 89(suppl 3), iii9-17.

[116] Yu, C.M, Lin, H, Ho, P.C, & Yang, H. Assessment of left and right ventricular systolic and diastolic synchronicity in normal subjects by tissue Doppler echocardiography and the effects of age and heart rate. Echocardiography. (2003)., 20(1), 19-27.

[117] Yalcin, F, Kaftan, A, Muderrisoglu, H, Korkmaz, M.E, Flachskampf, F, Garcia, M, & Thomas, J.D. Is Doppler tissue velocity during early left ventricular filling preload independent? Heart. (2002)., 87 (4), 336-339.

[118] Pela, G, Regolisti, G, Coghi, P, Cabassi, A, Basile, A, Cavatorta, A, Manca, C, & Borghetti, A. Effects of the reduction of preload on left and right myocardial velocities analysed by Doppler tissue echocardiography in healthy subjects. Eur J Echocardiogr. (2004)., 5(4), 262-271.

[119] Horton, K.D, Meece, R.W, & Hill, J.C. Assessment of the right ventricle by echocardiography: a primer for cardiac sonographers. J Am Soc Echocardiogr. (2009)., 22(7), 776-792.

[120] Puwanat, S, Priester, T.C, Mookadam, F, Bruce, C.J, Redfield, M.M, & Chandrasekaran, K. Right ventricular function in patients with heart failure and preserved ejection fraction. Eur J Echocardiogr. (2009)., 10(6), 733-737.

[121] Utsunomiya, H, Nakatani, S, Nishihira, M, Kanzaki, H, Kyotani, S, Nakanishi, N, Kihara, Y, & Kitakaze, M. Value of Estimated Right Ventricular Filling Pressure in Pre-

dicting Cardiac Events in Chronic Pulmonary Arterial Hypertension. J Am Soc Echocardiogr. (2009)., 22(12), 1368-1374.

[122] Kayser, H.W, van der Geest, R.J, van der Wall, E.E, Duchateau, C, & De Roos, A. Right ventricular function in patients after acute myocardial infarction assessed with phase contrast MR velocity mapping encoded in three directions. J Magn Reson Imaging. (2000)., 11(5), 471-475.

[123] Paelinck, B.P, De Roos, A, Bax, J.J, Bosmans, J.M, van der Geest, R.J, Dhondt, D, Parizel, P.M, Vrints, C.J, & Lamb, H.J. Feasibility of tissue magnetic resonance imaging: a pilot study in comparison with tissue Doppler imaging and invasive measurement. J Am Coll Cardiol. (2005)., 45(7), 1109-1116.

[124] Janda, S, Shahidi, N, Gin, K, & Swiston, J. Diagnostic accuracy of echocardiography for pulmonary hypertension: a systematic review and meta-analysis. Heart. (2011)., 97(8), 612-622.

[125] Sitbon, O, Humbert, M, Jais, X, Ioos, V, Hamid, A.M, Provencher, S, Garcia, G, Parent, F, Herve, P, & Simonneau, G. Long-term response to calcium channel blockers in idiopathic pulmonary arterial hypertension. Circulation. (2005)., 111(23), 3105–3111.